OPTIC TRACT FORMATION: RETINAL AXONS' INTERACTION WITH THEIR PIONEERS AND PEERS, AND A STRATEGY TO ANALYZE SPLICE VARIANTS OF GUIDANCE RECEPTOR MESSENGER RNAS

by

Mei Yee Law

A dissertation submitted to the faculty of
The University of Utah
in partial fulfillment of the requirements for the degree of

Doctor of Philosophy

Interdepartmental Neuroscience Program

The University of Utah

December 2011

The University of Utah Graduate School

STATEMENT OF DISSERTATION APPROVAL

The dissertation of **Mei Yee Law**

has been approved by the following supervisory committee members:

Chi-Bin Chien	, Chair	**7/6/2011** Date Approved
David J. Grunwald	, Member	**7/6/2011** Date Approved
Aloisia Schmid	, Member	**7/6/2011** Date Approved
Monica L. Vetter	, Member	**7/18/2011** Date Approved
Richard I. Dorsky	, Member	**7/18/2011** Date Approved

and by **Kristen A. Keefe**, Chair of the Department of **Interdepartmental Neuroscience Program**

and by Charles A. Wight, Dean of The Graduate School.

ABSTRACT

How neural connections are established spontaneously to generate a functioning nervous system remains an important question in the field of developmental biology. Axons and dendrites extended from various cell types have to form at the right place and right time to make appropriate connections. An enormous number of molecules is present in the developing embryos. Experimental analyses are further complicated by virtue of these molecules' ability to interact and affect the function of other molecules. I first set out to test the role of a cell biological mechanism—axon fasciculation—in guiding axon pathfinding within the zebrafish visual system. I then focused on the role of a transmembrane receptor, Robo2, and its splice variants in axon guidance.

In Chapter 1, I present some important questions in axon guidance and alternative splicing, along with reviews of factors involved in retinal axon guidance. I also introduce the roles of alternative splicing in increasing protein diversity and thus contributing to various responses in pathfinding along the axon trajectory.

Chapter 2 is a collaborative peer-reviewed paper published in *Development* showing that early-born retinal ganglion cells guide later-born cells within and outside of the eye.

In Chapter 3, I described my observation of *robo2* alternative splice forms in developing zebrafish embryos and my experiments using morpholinos to test the domains

functionally.

Finally, Chapter 4 discusses the findings and future directions of the studies.

TABLE OF CONTENTS

ACKNOWLEDGEMENTS

No words are ever enough to convey my gratitude towards all the people and the events that I have encountered along the steps of my life to make me who I am today.

I thank my mentor, Chi-Bin Chien, for the opportunity to join his lab. He has been extremely supportive towards my projects throughout my graduate career. His enthusiasm towards science and life is infectious. I am grateful for the good opportunities to learn a great deal from him through productive conversations at our meetings. His positive, determined, and humble attitudes are something I will always look up to in my life.

I also want to thank my committee members Richard Dorsky, David Grunwald, Alice Schmid, and Monica Vetter for being generous with their time, always asking stimulating questions and giving constructive suggestions to keep the project focused. I appreciate advice and encouragement from Joshua Bonkowsky, who always keeps his door open to discussions.

Without friends and good people in the lab, my graduate experience would not have been the same. They are Andrew Pittman, Renee Bend, Thao Nguyen, Amy Lim, Fabienne Poulain, John (Bull) Manfredi, Douglas Campbell, Jude Rosenthal, John Gaynes, Melissa Hardy, Coni Stacher, Kristen Kwan, Aaron Scoresby, Brooke Gaynes, Spencer Mangum, Nicholas Dambrauskas, LingYan Xing, and Tammy Stevenson. During my graduate career, I had the opportunity to become an office-mate and good

friend with Renee. Along with Renee, Thao, Amy and Fabienne, we often shared stories about our life with each other. I would also like to thank Esther Fujimoto, who recently passed away while I was revising my thesis, for all her generous help and advice about molecular cloning and about life.

I owe gratitude to my parents Law Kem Fong and Kheng Swe Yeat, who worked hard all their lives and always emphasized on the importance of good education to their children. Also thanks to my brothers and sister Hoe Yen, Hoe Thiam, and Ching Yee for continuous support from the opposite side of the globe. I am grateful to my husband, Kin Hoe Chow, for his unconditional love and support throughout my graduate career. Finally, sincere thanks and love to all of you.

CHAPTER 1

INTRODUCTION

Nervous system development and brain connectivity

There are an average of 100 billion neurons in the adult human brain, 950 thousand in honeybees, and 20 thousand in *Aplysia* (Pakkenberg and Gundersen, 1997; Menzel and Giurfa, 2001). These organisms share a common feature: for their brains to function, this enormous number of neurons must make appropriate connections with their targets. As the brain develops, each neuron sends its axon out to navigate through a complex environment, find its appropriate target, and make about 2000~5000 synaptic connections for appropriate signaling to occur. Growth cones, the structure at the most distal tip of the axon from the cell body, thus play an extremely important role in sniffing out the environment, detecting gradients of guidance cues along the way, and analyzing opposing signals to make guidance decisions, leading to downstream cytoskeleton reorganization. The decision of whether the growth cone is attracted, repelled, or stalled depends on the internal state and external cues of the growth cone, namely the expression of other coreceptors and molecules that can act to either suppress or enhance the signals. A previous encounter with the same guidance cue may have altered the growth cone's response by regulating its internal state. At the same time, a guidance decision can also be affected by the external state of the growth cone, including other membrane bound or secreted molecules in the extracellular matrix.

Several mechanisms have been proposed to guide growth cones in a complex environment (Raper and Mason, 2010). The first growth cones (pioneers) navigating in the naïve environment are sometimes found to contact intermediate targets, called guidepost cells, located along their trajectories (Bate, 1976; Bentley and Caudy, 1983a, 1983b). In return, these pioneers serve as a blueprint for later born neurons (followers), giving them guidance on a leg of the journey to their targets (Wilson et al., 1990). In addition to pioneer-follower guidance, axons sometimes are found to fasciculate with other axons taking the same route at the same time. This fasciculation interaction is not limited to neuron-neuron fasciculation but is also one of the many roles of glia in axon guidance (Learte and Hidalgo, 2007). Glial cells are often found at the intermediate targets. They can fasciculate with neurons for a short distance and secrete attractive or repulsive cues at the next intermediate target to guide axons. The first chemoaffinity hypothesis proposed by Roger Sperry stated that the postsynaptic surface presented cues that guide the axons to their proper targets (Sperry, 1963). Since then, many guidance molecules have been described, including the four best-studied "canonical" families of cues and receptors: Slit-Robo, Netrin-DCC/Unc5, Ephrin-Eph, and Semaphorin-Sema (Barton et al., 2004; Bashaw and Klein, 2010).

Despite the amount of attention on axon guidance research, there are still many open questions in the field. This comes as no surprise, given the complex nature of wiring in an organism. Following are some of the unanswered questions: Are pioneers important for large vertebrate axon tracts? What is the role of axon-axon interaction when axons are also challenged with axon guidance cues? These are addressed in Chapter 2. In Chapter 3,

I asked the questions: are *robo2* (*roundabout2*) alternate spliced forms regulated? Does splicing affect Robo2 function?

Defects in axon guidance and aberrant axon connectivity can result in various human disease conditions, including dyslexia, corpus callosum agenesis, L1 syndrome, Joubert syndrome and related disorders, horizontal gaze palsy with progressive scoliosis (HGPPS), Kallmann syndrome, albinism, congenital fibrosis of the extraocular muscles type 1, Duane retraction syndrome, and pontine tegmental cap dysplasia (Engle, 2010; Hannula-Jouppi et al., 2005). This makes the process of axon guidance not only very interesting, but also important to understand. Since it is unethical to use *Homo sapiens* in experiments, researchers rely on animal models to study this fundamental biological process.

Animal models have simpler nervous systems, allowing easier experimental manipulations. They are nevertheless useful for understanding the intricate process of axon guidance in the human brain due to the evolutionarily conserved roles of axon guidance cues. Zebrafish research was begun in the early 1970s by George Streisinger. The field has quickly flourished in less than four decades to include studies in both basic science and translational research. Here, I use the zebrafish as a model to study the guidance of retinal and other axons.

Zebrafish present an excellent tool for studying retinotectal axon guidance. First, zebrafish are vertebrates, which means they are phylogenically more closely related to humans than invertebrate models. They are easy to maintain, and zebrafish females can lay many eggs, making it easier to compare phenotype among many embryos across various time points. In addition, embryos are externally fertilized, rendering them

amenable to quick genetic manipulation by DNA, RNA, or morpholino injection. Morpholinos are short antisense oligo sequences with modified backbones that are often used to test gene functions. They create steric hindrance at exon-intron boundaries or at translation start sites to block splicing or protein translation. Coupled with transgenic lines expressing stable fluorescent proteins as cell type markers, they facilitate visualization of the effect of genetic manipulation within hours or days of development. The zebrafish embryo develops from a single cell into its mature body plan within 24 hours postfertilization (hpf) compared to 21 days in mice. Mechanical manipulations such as cell transplants, laser ablations, and mechanical ablations can also be applied to developing embryos to study what a group of cells later becomes or whether their offspring are required for normal zebrafish development. This also illustrates another advantage of using zebrafish, that the body is highly transparent during early development. With help of transgenic animals that specifically label the retinal ganglion cells (RGCs), such as *isl2b:GFP*^{zc7} and *brn3c:GFP*^{s356t}, we can greatly enhance the visualization of RGC axons in vivo.

Retinotectal axon guidance

The initial steps in developing a functional visual system involve proper guidance of the retinal axon to leave the eye at the optic disc and enter the optic nerve. The first RGC differentiation occurs at about 28 hpf (hours postfertilization) in the ventral-nasal part of the retina, followed by axon extension and exit from the retina at about 32 hpf. There are six major classes of neurons and one class of glial cells in a vertebrate eye. The retinal ganglion cell is the only cell type that extends axons outside the retina. Once they exit the eye, the early population of RGC axons begin their long journey navigating in the

brain by first crossing the optic chiasm at approximately 36 hpf and reaching the contralateral tectum at 48 hpf. Retinal axons are guided by extracellular guidance cues. In addition to the four major classes of axon guidance molecules—Slits, Netrins, Ephrins, and Semaphorins (Barton et al., 2004; Bashaw and Klein, 2010)—RGC axons can also be guided by axon fasciculation mediated by cell adhesion molecules.

Canonical cues

The Slits, the ligands for Robo receptors (Kidd et al., 1999), are thought to act as repulsive cues to channel retinal axons across the midline (Hutson and Chien, 2002; Plump et al., 2002). Heparan sulfate proteoglycans (HSPGs), which are known to bind to several axon guidance molecules, are necessary for Slit function. HSPGs are required for Slit's repulsion activity in Drosophila midline crossing (Steigemann et al., 2004). Inhibition of sulfation in Xenopus causes retinal axons to take aberrant routes to the tectum (Irie et al., 2002; Walz et al., 1997). Slit-induced repulsion in vitro is impaired when heparan sulfate is disrupted (Inatani et al., 2003; Piper et al., 2006). In zebrafish, *boxer;dackel* double mutants, which have very low HSPG levels, show guidance defects that phenocopy *astray*^{ti272z} (*robo2*) mutants (Lee et al., 2004). The heparan sulfate sulfotransferases, Hs2st and Hs6st, and *slit1* and *slit2* (*slit3* is not expressed in the retina) are expressed at the same time in mouse retina and optic chiasm (Erskine et al., 2000; Pratt et al., 2006). Results from Pratt et al. (2006) also point towards specificity of the heparan sulfate code in the Robo-Slit pathway. In the *hs2st*$^{-/-}$ mutant, retinal axons are disorganized at the optic chiasm, while in the *hs6st*$^{-/-}$ mutant, more retinal axons project to the contralateral eye.

Netrins are evolutionarily related to laminin. They have dual functions in axon guidance: the ligands can be both attractive and repulsive in vitro (Shewan et al., 2002). Generally, Netrins elicit an attractive response in growth cones when they bind to DCC (Delected in Colorectal Cancer) or neogenin but become repulsive when they interact with UNC-5/DCC receptors (Hong et al., 1999). Within the retina, retinal axons are attracted to the Netrin gradient expressed at the optic nerve head. Once they exit the retina, RGC axons become repelled by Netrin (Höpker et al., 1999). Consistent with these results, as RGC axons travel through the Xenopus optic tract, *netrin-1* is expressed deep in the neuroepithelium, but not superficially where RGC axons course (Shewan et al., 2002).

Ephrins/Ephs are involved in intraretinal navigation and in topographic mapping on the tectum (Birgbauer et al., 2000; Mann et al., 2004). In between retina and tectum, Ephrins/Ephs are thought to play a role in guiding ipsilateral retinal axons in animals with binocular vision. In Xenopus, chicks, and mouse embryos, Ephrin-Bs are expressed by radial glia at the optic chiasm and form a barrier to prevent a subpopulation of RGC axons (ventral-temporal) from entering the contralateral optic tract (Nakagawa et al., 2000; Williams et al., 2003).

Similar to Netrins, Semaphorins also have dual functions in axon guidance. Semaphorins can induce attractive or repulsive response in growth cones modulated by Semaphorin receptors—plexins and neuropilins—interacting with different members of the Ig superfamily of cell adhesion molecules (IgCAMs) (Bechara et al., 2007). In zebrafish retinal axons, Sema3d plays a role in guiding RGC axons at the optic chiasm (Sakai and Halloran, 2006).

Cell adhesion molecules

Cell adhesion molecules play an important role early on in the process of axon navigation. Retinal axons extending from their cell bodies in all quadrants of the retina travel towards the center of the retina, where the optic nerve exits through the optic nerve head. The optic nerve is formed by retinal axons that bundle together as a result of axon fasciculation, probably mediated through IgCAMs.

Ig superfamily CAMs represent an ancient group of molecules with diverged sequence and function. They possess characteristic immunoglobulin-like domains in the extracellular domain (Aricescu and Jones, 2007; Harpaz and Chothia, 1994). Ig superfamily CAMs that are expressed in developing axons can promote axon fasciculation (Barry et al., 2010; Key and Anderson, 1999; Stoeckli and Landmesser, 1995; Wolman et al., 2007), axon growth (Brittis et al., 1995; Grumet, 1992; Kristiansen et al., 2005), modulate growth cone response to guidance molecules (Suh et al., 2004), regulate topographic guidance of retinal axons on the superior colliculus (Buhusi et al., 2008), and affect retinotopic mapping of retinal axons (Buhusi et al., 2009). The neural cell adhesion molecule (NCAM) is the first CAM in the Ig-superfamily that was shown to mediate retinal ganglion cell adhesion (Hoffman et al., 1982). Alternative splicing of NCAM gives rise to three splice forms in zebrafish, each capable of being polysialylated. Sialic acid addition to NCAM during developmental stages confers on axons the ability to migrate and abrogate NCAM adhesion during axon outgrowth via steric hindrance (Johnson et al., 2005). For example, loss of polysialic acid in mice leads to severe anatomical disorganization of forebrain tissue, aberrant cell death, and glial cell

differentiation as a consequence of defects in cell migration and differentiation (Angata et al., 2007).

Zebrafish L1.1 and L1.2—duplicated orthologs of mouse L1—and NrCAM are members of the L1 subfamily. L1.1 and L1.2 have been shown to have overlapping expression in postmitotic neurons during zebrafish development (Tongiorgi et al., 1995). When L1 was blocked with Fab fragments in developing rat retina, the guidance and rate of axonal growth were affected (Brittis et al., 1995). NrCAM is another IgCAM that has shown to be expressed in the RGC axons but not the cell body during its extension. Perturbation of NrCAM in chick retina flat-mounts by specific Fab fragments leads to larger and more complex growth cones and aberrant projection in the retina. It also results in slower chick retinal axon growth rate ex vivo (Zelina et al., 2005). The function of L1 is not expressed until after 37 hpf (Appendix) whereas NrCAM is unlikely to have a role (not expressed in the early retina development) in zebrafish.

Neurolin and neurolin-like cell adhesion molecule (NLCAM) (also called ALCAM and neurolin-b, respectively) are another example of a duplicated gene pair, and belong to the activated leukocyte cell adhesion molecule (ALCAM) subfamily of Ig-CAM. Neurolin and NLCAM have five extracellular Ig domains, a transmembrane domain, and a conserved cytoplasmic domain with about 45% similarity to each other at the protein level (Mann et al., 2006). It forms homophilic or heterophilic interactions with other soluble or membrane-bound molecules via its second Ig domain (Drees et al., 2008) to mediate tumor metastasis, axon guidance, and fasciculation. Neurolin and NLCAM are expressed in zebrafish eyes during the period of retinal axon elongation in the central nervous system. In cases where neurolin function is disrupted, mouse motor and retinal

axons travel in looser bundles and sometimes make pathfinding mistakes (Weiner et al., 2004). In zebrafish, morpholino knockdown of neurolin results in motor axons defasciculation and smaller eyes, owing to a severe delay in RGC differentiation (Diekmann and Stuermer, 2009; Ott et al., 2001). NLCAM mediates cell migration during optic vesicle morphogenesis and retinal axon pathfinding in zebrafish (Brown et al., 2010; Diekmann and Stuermer, 2009).

Other cues

In addition to the four major classes of guidance cues and cell adhesion molecules mentioned above, RGC axon navigation can also be fine-tuned by many extracellular cues. Among them are the growth factors. For instance, fibroblast growth factor receptor regulates *slit1* and *sema3A* expression in Xenopus, which in turn affects repulsive responses in growth cones (Atkinson-Leadbeater et al., 2010). Vascular endothelial growth factor is another example of a growth factor that has been recently identified to affect retinal axon guidance at the optic chiasm, by binding to Neuropilin-1 (Erskine et al., 2011). At all points in the retinotectal pathway, many guidance molecules likely surround retinal axons, together orchestrating and fine-tuning the growth cone response.

Although guidance cues and axon fasciculation are each known to be important in axon navigation, a question that has not been addressed is: will guidance cues overshadow the effect of axon fasciculation, or vice versa? In particular, what are the relative roles of pioneer-follower interactions and guidance cues in a large vertebrate axon tract? Furthermore, what mediates pioneer-follower interactions in a large vertebrate axon tract?

In Chapter 2, we set out to test the importance of a key guidance system (Slit-Robo signaling) in the context of the intact environment in vivo. We showed that during zebrafish retinal axon outgrowth, isotypic axon-axon interaction plays an equally important role as guidance cue-receptor interactions in axon pathfinding from the eye to the tectum. For the earlier step of guidance within the eye, pioneer axons play a key role. When differentiation of pioneer RGCs is blocked with *ath5* morpholino, follower retinal axons are trapped and make aberrant projections inside the eye. Within the eye, when supplied with pioneer retinal axons, follower axons' trajectories in *ath5* morphants are affected by the genotype of pioneer axons (Pittman et al., 2008). These results suggest an axon-axon mediated interaction that helps axons to fasciculate and form a tight bundle when traveling in a novel environment. A future goal is to investigate functionally IgCAMs that may play a role in retinal axon fasciculation based on their expression patterns during various stages of axon outgrowth. These IgCAMs include NCAM, L1.1, L1.2, NrCAM, neurolin, and NLCAM (Appendix).

Robo function, signaling, and splicing

The *robo* gene was first identified in a Drosophila screen for genes that control midline crossing in the central nervous system (Kidd et al., 1998; Seeger et al., 1993). Commisural axons in *robo* mutants cross multiple times at the midline while in the absence of Slit, all commissural axons collapse at the midline. In *commisureless* (*comm*) mutants, commissural axons extend a short distance towards the midline and stop before entering. Instead of crossing the midline, axons turn rostrocaudally and navigate in longitudinal axon pathways on the ipsilateral side. In contrast, commissural axons in *robo* mutants cross the midline multiple times and longitudinal pathways collapse closer

together. Identified in biochemical purification and genetic linkage analysis, Slit is a large secreted molecule expressed by midline glia cells that acts as a short-range repellent ligand which inhibits ectopic midline crossing by Robo-expressing commissural axons (Brose et al., 1999; Kidd et al., 1999; Wang et al., 1999). Several years later, it was discovered that flies have three Robo genes: Robo1 (Robo), Robo2, and Robo3 (Simpson et al., 2000). Robo1 is expressed in both longitudinal and commissural axons, but only commissural axons express Comm (Keleman et al., 2002). Comm negatively regulates Robo1 by endosomal sorting to the late endocytic pathway, thereby reducing Slit sensitivity of these axons (Simpson et al., 2000). After crossing the midline, Robo1 expression is increased in commissural axons to prevent axon recrossing. There are three lateral zones in longitudinal axons (longitudinal fascicles), with different combinations of the "Robo code" determining the lateral positioning of the longitudinal axon pathways (Rajagopalan, Nicolas, et al., 2000; Rajagopalan, Vivancos, et al., 2000; Simpson et al., 2000; Spitzweck et al., 2010). Axons in the most medial longitudinal fascicle express only Robo1, axons in the intermediate fascicle express Robo1 and Robo3, while axons in the most lateral fascicle express Robo1, 2, and 3. Structural differences in the intracellular domain, and in the expression profile of the 3 Robos, were proposed to explain their different responses to their ligand, Slit.

A series of gene duplication events during evolution has given rise to one Robo gene (Sax-3) in C. elegans, three in Drosophila (Robo1-3), four Robos in zebrafish (Robo1-4), and four Robos in mammals (Robo1/Dutt, Robo2, Robo3/Rig1, Robo4). All Robo family receptors have five immunoglobulin (IgG) repeats and three fibronectin III (FNIII)-like repeats in their extracellular domain (Kidd et al., 1998; Zallen et al., 1998),

except murine and human *robo4* which have only two IgG and FNIII domains (Huminiecki et al., 2002) and zebrafish *robo4* which has three IgG and two FNIII domains (Park et al., 2003).These different Robo receptors have overlapping and distinct expressions and functions during embryonic development and in mature organisms. However, functions of orthologous genes are often conserved across different species. As in Drosophila, Robo functions in midline crossing in vertebrates. In *robo3* (also known as *rig-1*) mouse mutants, commissural axons fail to cross the midline (Barber et al., 2009; Sabatier et al., 2004). Human patients with *robo3* mutations, similar to their murine counterparts, develop HGPPS, characterized by an absence of hindbrain axon crossing that results in a horizontal eye movement disorder (Jen et al., 2004; Renier et al., 2010).

Robos also function in retinal axon guidance. Robo1 is expressed in the chick inner nuclear layer and a subset of cells during retina development (Huang et al., 2009). In the murine visual system, Robo2 receptor is the predominant and earliest expressing Robo, with Robo1 expressed to a lesser extent and later (Erskine et al., 2000; Plachez et al., 2008; Ringstedt et al., 2000). Robo1 is expressed in the retinal marginal zone and shows low and scattered expression in the presumptive RGC layer; it may be involved in intraretinal development (Ringstedt et al., 2000). After leaving the eye, the optic nerve bifurcates at the optic chiasm to enter the ipsilateral and contralateral optic tracts in a highly specific choice of pathway. This choice of pathway persists into adulthood (Sretavan, 1990). Both *robo1* and *robo2* are expressed in retina, optic nerve, optic chiasm, and along the entire optic tract as the RGC axons grow. Robo1 knockout mice have an optic chiasm that is widened along the rostro-caudal axis, and ectopic projections in the ventral diencephalon. Robo2 mutant mice have a much stronger defect in the visual

pathway, with an expanded optic chiasm, and aberrant projections to the contralateral optic nerve and forebrain (Plachez et al., 2008). Collectively, these results show that Robo2 plays a major role in retinal axon pathfinding and targeting to the superior colliculus in the mouse.

Zebrafish Robo2 acts alone to control retinal axon pathfinding and targeting to the tectum (Fricke et al., 2001), unlike the mouse system where Robo1 and Robo2 are both important for visual system development. Zebrafish Robo2 comprises five IgG domains and three FNIII-repeats in its ectodomain with a long cytoplasmic tail. *robo2* is expressed in the RGC layer at 36 hpf and its expression persists throughout retinal axon pathfinding. It is also strongly expressed in the tectum (the homolog of the mammalian superior colliculus), with weaker staining of *robo1* and staining of *robo3* in a superficial subset of cells (Lee et al., 2001; Fricke et al., 2001). The *astray* mutant, isolated in a large-scale screen for mutants defective in retinotectal pathfinding (Trowe et al., 1996), was later identified to have a defect in zebrafish *robo2* (Fricke et al., 2001). The ast^{ti272z} allele encodes an early nonsense mutation before the second FNIII repeat in the extracellular domain of the *robo2* gene. In these mutants, retinal axons leave the eye at the optic nerve head but make retinotectal pathfinding mistakes at various choice points outside of the eye: right after exiting the eye, at the optic chiasm, and before entering the tectum. In addition, *astray* mutants have defects in olfactory receptor neuron targeting (Miyasaka et al., 2005), in spinal cord commissural primary ascending neuron pathfinding (Bonner and Dorsky, unpublished), and in RGC axon arborization on the tectum (Campbell et al., 2007).

Robo signaling

A comparison of Robo receptor sequences between vertebrates and invertebrates revealed a highly conserved ectodomain and a very diverged endodomain. In the ectodomain, Robo-Slit interaction occurs between the second Slit LRR domain and the first two Robo Ig domains (Chen et al., 2001; Morlot et al., 2007; Nguyen Ba-Charvet et al., 2001). Within the endodomain, there are four short conserved cytoplasmic (CC) motifs shared between invertebrates and vertebrates: CC0, CC1, CC2, and CC3 (Bashaw et al., 2000; Kidd et al., 1998; Wong et al., 2001). The CC0 and CC1 motifs are tyrosine phosphorylation sites in vitro while CC2 and CC3 are proline-rich motifs likely to undergo protein-protein interactions. Enabled (Ena), an evolutionarily conserved protein that has been implicated in actin cytoskeleton regulation, binds to the CC2 and possibly CC1 domains, serving an important role in Robo repulsive axon guidance in Drosophila. However, Ena function cannot account for all Robo repulsive activity (Bashaw et al., 2000; Yu et al., 2002). Abelson tyrosine kinase (Abl), an upstream regulator of Ena, binds to the Robo CC3 domain (Rhee et al., 2002). Upon activation by Slit binding to Robo, Abl phosphorylates tyrosine residues in both CC0 and CC1 and downregulates Robo activity (Bashaw et al., 2000). Upon Slit activation, Robo also inhibits N-cadherin cell-cell adhesion by forming a complex with Abl and N-cad (Rhee et al., 2002). Abl recruits Cables, an adaptor protein, which in turn forms a complex with N-cadherin-associated Cdk5 and β-catenin. Cables brings Abl to phosphorylate β-catenin. The phosphorylated form of β-catenin loses affinity with N-cadherin, translocates and activates transcription in the nucleus (Rhee et al., 2007). Both Ena and Abl function downstream of the Robo receptor and play important functions in actin cytoskeleton

assembly and disassembly. In addition to binding to Robo, Abl and Ena also physically interact with the Netrin receptor Frazzled (Fra), suggesting a role in coordinating attraction and repulsion cues in *Drosophila* midline axon guidance (Forsthoefel et al., 2005).

Rho-family GTPases have a conserved role in regulating the dynamics of the actin and microtubule cytoskeleton (Hall and Lalli, 2010) that can be inhibited by GTPase-activating proteins (GAPs) and stimulated by guanine nucleotide exchange factors (GEF). Thus it is not surprising that members of the Rho-GAP family, CrGAP/Vilse and Slit-Robo GAP (srGAP), interact directly with the Robo cytoplasmic domain. Drosophila CrGAP/Vilse physically and genetically interacts with the CC2 domain and functions to mediate axon repulsion in midline neurons (Hu et al., 2005) and tracheal cells and axons (Lundström et al., 2004). srGAP1 and srGAP2 were identified in a yeast-two hybrid screen to identify the signal transduction mechanism that interacts with rat Robo1 in the brain (Wong et al., 2001). The SH3 domain of srGAP binds to the CC3 domain on Robo1 (Li et al., 2006; Wong et al., 2001). Slit binding to Robo1 increases srGAP1 interaction with Robo1 and causes downstream inhibition of Cdc42. The inactive form of Cdc42 leads to a reduction of N-WASP (Neuronal Wiskott-Aldrich Syndrome protein) and Arp2/3 complex activities. Reduction of the Arp2/3 complex then translates into a decrease in actin polymerization on the side of the cell proximal to high Slit concentration. Dock is another adaptor protein that binds to the Robo CC2 and CC3 motifs via its SH3 domains in Drosophila (Fan et al., 2003). Dock is likely to couple with Rac and Pak as a protein complex in response to Robo activation. This leads to the downstream response of actin cytoskeleton regulation and axon repulsion.

Although Robo interacting partners have been identified, one of the open questions remaining is, how does Robo2 signal in vivo in vertebrate retinal axon guidance? My experiments detailed in Chapter 3 represent the first study to correlate functions of Robo2 intracellular domains with retinal axon guidance, in vivo.

Alternative splicing of Robo receptors

The same genomic sequence for a gene can sometimes give rise to different transcripts. This occurs through a process called alternative splicing, which takes place at the pre-mRNA level. It is estimated that close to 90% of human genes are alternatively spliced (Luco et al., 2011). Alternative splicing plays an important role in increasing protein diversity from a finite pool of genes encoded in the genome. Signals from these proteins expressed at the same place are transduced into cells to fine-tune their output response to affect differentiation, development, and disease (Luco et al., 2011). The fly DSCAM (Down syndrome cell adhesion molecule) gene remains the most intriguing example of alternative splicing due to its ability to encode more than 38,000 different proteins (May et al., 2011). Mature mRNA sequences vary from each other depending on the exon-intron boundaries used and cryptic splice sites that are activated (Luco et al., 2011).

Several Robo3 splice isoforms have been reported (Camurri et al., 2005; Challa et al., 2001; Yuan et al., 1999). Two particular splice variants generated by differential intron retention create two Robo3 isoforms: Robo3.1 and Robo3.2 (Chen et al., 2008). Both forms are present in mouse commissural axons. Robo3.1 is required for inhibiting Slit repulsion in precrossing axons while Robo3.2 is required for axons to be expelled from the midline after crossing (Chen et al., 2008). These experiments showed that,

although arising from the same gene, splice isoforms can have distinct functions in the same neuron.

Zebrafish *robo2* plays a crucial role in controlling retinal axon navigation during extension across the brain (Fricke et al., 2001). *robo2* mRNA is expressed in the RGCs as their axons navigate throughout their pathway: after exiting the eye, at the midline (chiasm), and entering the tectum (Fricke et al., 2001; Lee et al., 2001). Timelapse and fixed analysis of *robo2* (*astray*) mutants showed that some retinal axons stray from the wildtype pathway and venture into other areas of the brain after exiting from the eye, at the midline, or before entering the tectum (Hutson and Chien, 2002). In addition, a lack of Robo2 in the retinal axon growth cone results in an increase in arborization on the tectum (Campbell et al., 2007). In summary, Robo2 in retinal axons has many roles during development.

How can a single gene such as *robo2* mediate different responses at various choice points? One possibility is that it generates multiple protein forms. Several Robo2 splice isoforms have been identified in human, mouse, and zebrafish (Dalkic et al., 2006; Yue et al., 2006). Robo2 in human is present in two forms, Robo2a and Robo2b, with different N termini. Robo2a and Robo2b utilize different 5' UTR and translational start sites, but the mature proteins only differ from each other in four amino acids (Yue et al., 2006). Both isoforms are expressed in fetal human brains from 11 weeks to 42 weeks gestation. Expression profiling comparing brain tissue and other tissue revealed that Robo2a is expressed predominantly in fetal brains whereas Robo2b is also expressed in adult brain, heart, kidney, colon, and all other tissue examined in addition to fetal human brains. Although this research was not able to identify Robo2 functions in developing

human embryos, the expression patterns suggested that both isoforms have distinct functions and that Robo2a is necessary in the developing fetal brain. It is more feasible to study gene functions in zebrafish using morpholinos or transgenic animals. Consistent with human Robo2, mouse Robo2a and 2b have 4 amino acids' difference in the N-terminus. This study also identified two alternatively employed exons (a novel 126bp exon between Ensembl exons 20 and 21 and the 237bp exon 25) (Yue et al., 2006). The 126bp exon in the mouse corresponds to exon 23 in the zebrafish, which is alternately spliced and only differs by 5/42 amino acids from the mouse. Interestingly, although it is very conserved in human genomic sequence (Figure 3.1), the same alternative splice form has not been reported in human cDNA.

Previous preliminary data from our lab suggested that some *robo2* exons may be alternatively spliced in zebrafish larvae. My goal in Chapter 3 was to answer the questions: (1) are alternate splice forms regulated? and (2) does splicing affect Robo2 function?

Having summarized mechanisms of axon guidance, functions of Robo receptors, and alternative splicing in Chapter 1, I will discuss experiments to look at pioneer-follower guidance in Chapter 2. I then discuss the regulation and potential function of Robo2 alternate splice forms in Chapter 3. Chapter 4 summarizes findings in the two previous chapters and discusses future directions.

Reference

Angata, K., Huckaby, V., Ranscht, B., Terskikh, A., Marth, J. D., and Fukuda, M. (2007). Polysialic acid-directed migration and differentiation of neural precursors are essential for mouse brain development. *Mol. Cell. Biol.*, **27**, 6659-6668.

Aricescu, A. R. and Jones, E. Y. (2007). Immunoglobulin superfamily cell adhesion molecules: zippers and signals. *Curr. Opin. Cell Biol.*, **19**, 543-550.

Atkinson-Leadbeater, K., Bertolesi, G. E., Hehr, C. L., Webber, C. A., Cechmanek, P. B., and McFarlane, S. (2010). Dynamic expression of axon guidance cues required for optic tract development is controlled by fibroblast growth factor signaling. *J. Neurosci.*, **30**, 685 -693.

Barber, M., Di Meglio, T., Andrews, W. D., Hernandez-Miranda, L. R., Murakami, F., Chedotal, A., and Parnavelas, J. G. (2009). The role of Robo3 in the development of cortical interneurons. *Cerebral Cortex*, **19**, i22-i31.

Barry, J., Gu, Y., and Gu, C. (2010). Polarized targeting of L1-CAM regulates axonal and dendritic bundling in vitro. *Eur. J. Neurosci.*, **32**, 1618-1631.

Barton, W. A., Himanen, J.-P., Antipenko, A., and Nikolov, D. B. (2004). Structures of axon guidance molecules and their neuronal receptors. *Adv. Protein Chem.,* **68**, 65-106.

Bashaw, G. J., Kidd, T., Murray, D., Pawson, T., and Goodman, C. S. (2000). Repulsive axon guidance: Abelson and Enabled play opposing roles downstream of the roundabout receptor. *Cell*, **101**, 703-715.

Bashaw, G. J. and Klein, R. (2010). Signaling from axon guidance receptors. *Cold Spring Harb. Perspect. Biol.*, **2**, a001941.

Bate, C. M. (1976). Pioneer neurones in an insect embryo. *Nature*, **260**, 54-56.

Bechara, A., Falk, J., Moret, F., and Castellani, V. (2007). Modulation of semaphorin signaling by Ig superfamily cell adhesion molecules. *Adv. Exp. Med. Biol.*, **600**, 61-72.

Bedell, V. M., Yeo, S.-Y., Park, K. W., Chung, J., Seth, P., Shivalingappa, V., Zhao, J., Obara, T., Sukhatme, V. P., Drummond, I. A., Li, D. Y. and Ramchandran, R. (2005). Roundabout4 is essential for angiogenesis in vivo. *Proc. Natl. Acad. Sci. U.S.A.*, **102**, 6373-6378.

Bentley, D. and Caudy, M. (1983a). Navigational substrates for peripheral pioneer growth cones: limb-axis polarity cues, limb-segment boundaries, and guidepost neurons. *Cold Spring Harb. Symp. Quant. Biol.*, **48 Pt 2**, 573-585.

Bentley, D. and Caudy, M. (1983b). Pioneer axons lose directed growth after selective killing of guidepost cells. *Nature*, **304**, 62-65.

Birgbauer, E., Cowan, C. A., Sretavan, D. W., and Henkemeyer, M. (2000). Kinase independent function of EphB receptors in retinal axon pathfinding to the optic disc from dorsal but not ventral retina. *Development*, **127**, 1231-1241.

Brittis, P. A., Lemmon, V., Rutishauser, U., and Silver, J. (1995). Unique changes of ganglion cell growth cone behavior following cell adhesion molecule perturbations: a time-lapse study of the living retina. *Mol. Cell. Neurosci.*, **6**, 433-449.

Brose, K., Bland, K. S., Wang, K. H., Arnott, D., Henzel, W., Goodman, C. S., Tessier-Lavigne, M., and Kidd, T. (1999). Slit proteins bind Robo receptors and have an evolutionarily conserved role in repulsive axon guidance. *Cell*, **96**, 795-806.

Brown, K. E., Keller, P. J., Ramialison, M., Rembold, M., Stelzer, E. H. K., Loosli, F., and Wittbrodt, J. (2010). Nlcam modulates midline convergence during anterior neural plate morphogenesis. *Dev. Biol.*, **339**, 14-25.

Buhusi, M., Demyanenko, G. P., Jannie, K. M., Dalal, J., Darnell, E. P. B., Weiner, J. A., and Maness, P. F. (2009). ALCAM regulates mediolateral retinotopic mapping in the superior colliculus. *J. Neurosci.*, **29**, 15630-15641.

Buhusi, M., Schlatter, M. C., Demyanenko, G. P., Thresher, R., and Maness, P. F. (2008). L1 interaction with ankyrin regulates mediolateral topography in the retinocollicular projection. *J. Neurosci.*, **28**, 177-188.

Campbell, D. S., Stringham, S. A., Timm, A., Xiao, T., Law, M.-Y., Baier, H., Nonet, M. L., and Chien, C.-B. (2007). Slit1a inhibits retinal ganglion cell arborization and synaptogenesis via Robo2-dependent and -independent pathways. *Neuron*, **55**, 231-245.

Camurri, L., Mambetisaeva, E., Davies, D., Parnavelas, J., Sundaresan, V., and Andrews, W. (2005). Evidence for the existence of two Robo3 isoforms with divergent biochemical properties. *Mol. Cell. Neurosci.*, **30**, 485-493.

Challa, A. K., Beattie, C. E., and Seeger, M. A. (2001). Identification and characterization of roundabout orthologs in zebrafish. *Mech. Dev*, **101**, 249-253.

Chen, J. H., Wen, L., Dupuis, S., Wu, J. Y., and Rao, Y. (2001). The N-terminal leucine-rich regions in Slit are sufficient to repel olfactory bulb axons and subventricular zone neurons. *J. Neurosci.*, **21**, 1548-1556.

Chen, Z., Gore, B. B., Long, H., Ma, L., and Tessier-Lavigne, M. (2008). Alternative splicing of the Robo3 axon guidance receptor governs the midline switch from attraction to repulsion. *Neuron*, **58**, 325-332.

Dalkic, E., Kuscu, C., Sucularli, C., Aydin, I. T., Akcali, K. C., and Konu, O. (2006). Alternatively spliced Robo2 isoforms in zebrafish and rat. *Dev. Genes Evol.*, **216**, 555-563.

Diekmann, H. and Stuermer, C. A. O. (2009). Zebrafish neurolin-a and -b, orthologs of ALCAM, are involved in retinal ganglion cell differentiation and retinal axon pathfinding. *J. Comp. Neurol.*, **513**, 38-50.

Drees, C., Stürmer, C. A. O., Möller, H. M., and Fritz, G. (2008). Expression and purification of neurolin immunoglobulin domain 2 from Carrassius auratus (goldfish) in Escherichia coli. *Protein Expression Purif.*, **59**, 47-54.

Engle, E. C. (2010). Human genetic disorders of axon guidance. *Cold Spring Harb. Perspect. Biol.*, **2**, a001784.

Erskine, L., Reijntjes, S., Pratt, T., Denti, L., Schwarz, Q., Vieira, J. M., Alakakone, B., Shewan, D., and Ruhrberg, C. (2011). VEGF signaling through Neuropilin 1 guides commissural axon crossing at the optic chiasm. *Neuron*, **70**, 951-965.

Erskine, L., Williams, S. E., Brose, K., Kidd, T., Rachel, R. A., Goodman, C. S., Tessier-Lavigne, M., and Mason, C. A. (2000). Retinal ganglion cell axon guidance in the mouse optic chiasm: expression and function of Robos and Slits. *J. Neurosci.*, **20**, 4975 -4982.

Fan, X., Labrador, J. P., Hing, H., and Bashaw, G. J. (2003). Slit stimulation recruits Dock and Pak to the Roundabout receptor and increases Rac activity to regulate axon repulsion at the CNS midline. *Neuron*, **40**, 113-127.

Forsthoefel, D. J., Liebl, E. C., Kolodziej, P. A., and Seeger, M. A. (2005). The Abelson tyrosine kinase, the Trio GEF and Enabled interact with the Netrin receptor Frazzled in Drosophila. *Development*, **132**, 1983-1994.

Fricke, C., Lee, J. S., Geiger-Rudolph, S., Bonhoeffer, F., and Chien, C.-B. (2001). Astray, a zebrafish roundabout homolog required for retinal axon guidance. *Science*, **292**, 507-510.

Grumet, M. (1992). Structure, expression, and function of Ng-CAM, a member of the immunoglobulin superfamily involved in neuron-neuron and neuron-glia adhesion. *J. Neurosci. Res.*, **31**, 1-13.

Hall, A. and Lalli, G. (2010). Rho and Ras GTPases in axon growth, guidance, and branching. *Cold Spring Harb. Perspect. Biol.*, **2**, a001818.

Hannula-Jouppi, K., Kaminen-Ahola, N., Taipale, M., Eklund, R., Nopola-Hemmi, J., Kääriäinen, H., and Kere, J. (2005). The axon guidance receptor gene ROBO1 is a candidate gene for developmental dyslexia. *PLoS Genet.*, **1**, e50.

Harpaz, Y. and Chothia, C. (1994). Many of the immunoglobulin superfamily domains in cell adhesion molecules and surface receptors belong to a new structural set which is close to that containing variable domains. *J. Mol. Biol.*, **238**, 528-539.

Hoffman, S., Sorkin, B. C., White, P. C., Brackenbury, R., Mailhammer, R., Rutishauser, U., Cunningham, B. A., and Edelman, G. M. (1982). Chemical characterization of a neural cell adhesion molecule purified from embryonic brain membranes. *J. Biol. Chem.*, **257**, 7720-7729.

Hong, K., Hinck, L., Nishiyama, M., Poo, M. M., Tessier-Lavigne, M., and Stein, E. (1999). A ligand-gated association between cytoplasmic domains of UNC5 and DCC family receptors converts netrin-induced growth cone attraction to repulsion. *Cell*, **97**, 927-941.

Hu, H., Li, M., Labrador, J.-P., McEwen, J., Lai, E. C., Goodman, C. S., and Bashaw, G. J. (2005). Cross GTPase-activating protein (CrossGAP)/Vilse links the Roundabout receptor to Rac to regulate midline repulsion. *Proc. Natl. Acad. Sci. U.S.A.*, **102**, 4613-4618.

Huang, L., Yu, W., Li, X., Niu, L., Li, K., and Li, J. (2009). Robo1/robo4: different expression patterns in retinal development. *Exp. Eye Res.*, **88**, 583-588.

Huminiecki, L., Gorn, M., Suchting, S., Poulsom, R., and Bicknell, R. (2002). Magic Roundabout is a new member of the Roundabout receptor family that is endothelial specific and expressed at sites of active angiogenesis. *Genomics*, **79**, 547-552.

Hutson, L. D. and Chien, C.-B. (2002). Pathfinding and error correction by retinal axons: the role of astray/robo2. *Neuron*, **33**, 205-217.

Inatani, M., Irie, F., Plump, A. S., Tessier-Lavigne, M., and Yamaguchi, Y. (2003). Mammalian brain morphogenesis and midline axon guidance require heparan sulfate. *Science*, **302**, 1044 -1046.

Irie, A., Yates, E. A., Turnbull, J. E., and Holt, C. E. (2002). Specific heparan sulfate structures involved in retinal axon targeting. *Development*, **129**, 61 -70.

Jen, J. C., Chan, W.-M., Bosley, T. M., Wan, J., Carr, J. R., Rüb, U., Shattuck, D., Salamon, G., Kudo, L. C., Ou, J., et al. (2004). Mutations in a human ROBO gene disrupt hindbrain axon pathway crossing and morphogenesis. *Science*, **304**, 1509-1513.

Johnson, C. P., Fujimoto, I., Rutishauser, U., and Leckband, D. E. (2005). Direct evidence that neural cell adhesion molecule (NCAM) polysialylation increases intermembrane repulsion and abrogates adhesion. *J. Biol. Chem.*, **280**, 137-145.

Keleman, K., Rajagopalan, S., Cleppien, D., Teis, D., Paiha, K., Huber, L. A., Technau, G. M., and Dickson, B. J. (2002). Comm sorts robo to control axon guidance at the Drosophila midline. *Cell*, **110**, 415-427.

Key, B. and Anderson, R. B. (1999). Neuronal pathfinding during development of the rostral brain in Xenopus. *Clin. Exp. Pharmacol. Physiol.*, **26**, 752-754.

Kidd, T., Bland, K. S., and Goodman, C. S. (1999). Slit is the midline repellent for the robo receptor in Drosophila. *Cell*, **96**, 785-794.

Kidd, T., Brose, K., Mitchell, K. J., Fetter, R. D., Tessier-Lavigne, M., Goodman, C. S., and Tear, G. (1998). Roundabout controls axon crossing of the CNS Midline and defines a novel subfamily of evolutionarily conserved guidance receptors. *Cell*, **92**, 205-215.

Kristiansen, L. V., Velasquez, E., Romani, S., Baars, S., Berezin, V., Bock, E., Hortsch, M., and Garcia-Alonso, L. (2005). Genetic analysis of an overlapping functional requirement for L1- and NCAM-type proteins during sensory axon guidance in Drosophila. *Mol. Cell. Neurosci.*, **28**, 141-152.

Learte, A. R. and Hidalgo, A. (2007). The role of glial cells in axon guidance, fasciculation and targeting. *Adv. Exp. Med. Biol.*, **621**, 156-166.

Lee, J.-S., Ray, R., and Chien, C.-B. (2001). Cloning and expression of three zebrafish roundabout homologs suggest roles in axon guidance and cell migration. *Dev. Dyn.*, **221**, 216-230.

Lee, J.-S., von der Hardt, S., Rusch, M. A., Stringer, S. E., Stickney, H. L., Talbot, W. S., Geisler, R., Nüsslein-Volhard, C., Selleck, S. B., Chien, C.-B., Roehl, H. (2004). Axon sorting in the optic tract requires HSPG synthesis by ext2 (dackel) and extl3 (boxer). *Neuron*, **44**, 947-960.

Li, X., Chen, Y., Liu, Y., Gao, J., Gao, F., Bartlam, M., Wu, J. Y., and Rao, Z. (2006). Structural basis of Robo proline-rich motif recognition by the srGAP1 Src homology 3 domain in the Slit-Robo signaling pathway. *J. Biol. Chem.*, **281**, 28430-28437.

Luco, R. F., Allo, M., Schor, I. E., Kornblihtt, A. R., and Misteli, T. (2011). Epigenetics in alternative pre-mRNA splicing. *Cell*, **144**, 16-26.

Lundström, A., Gallio, M., Englund, C., Steneberg, P., Hemphälä, J., Aspenström, P., Keleman, K., Falileeva, L., Dickson, B. J., and Samakovlis, C. (2004). Vilse, a conserved Rac/Cdc42 GAP mediating Robo repulsion in tracheal cells and axons. *Genes Dev.*, **18**, 2161 -2171.

Mann, C. J., Hinits, Y., and Hughes, S. M. (2006). Comparison of neurolin (ALCAM) and neurolin-like cell adhesion molecule (NLCAM) expression in zebrafish. *Gene Expression Patterns*, **6**, 952-963.

Mann, F., Harris, W. A., and Holt, C. E. (2004). New views on retinal axon development: a navigation guide. *Int. J. Dev. Biol.*, **48**, 957-964.

May, G. E., Olson, S., McManus, C. J., and Graveley, B. R. (2011). Competing RNA secondary structures are required for mutually exclusive splicing of the Dscam exon 6 cluster. *RNA*, **17**, 222-229.

Menzel, R. and Giurfa, M. (2001). Cognitive architecture of a mini-brain: the honeybee. *Trends Cogn. Sci. (Regul. Ed.)*, **5**, 62-71.

Miyasaka, N., Sato, Y., Yeo, S.-Y., Hutson, L. D., Chien, C.-B., Okamoto, H., and Yoshihara, Y. (2005). Robo2 is required for establishment of a precise glomerular map in the zebrafish olfactory system. *Development*, **132**, 1283 -1293.

Morlot, C., Thielens, N. M., Ravelli, R. B. G., Hemrika, W., Romijn, R. A., Gros, P., Cusack, S., and McCarthy, A. A. (2007). Structural insights into the Slit-Robo complex. *Proc. Natl. Acad. Sci. U.S.A.*, **104**, 14923 -14928.

Nakagawa, S., Brennan, C., Johnson, K. G., Shewan, D., Harris, W. A., and Holt, C. E. (2000). Ephrin-B regulates the Ipsilateral routing of retinal axons at the optic chiasm. *Neuron*, **25**, 599-610.

Nguyen Ba-Charvet, K. T., Brose, K., Ma, L., Wang, K. H., Marillat, V., Sotelo, C., Tessier-Lavigne, M., and Chédotal, A. (2001). Diversity and specificity of actions of Slit2 proteolytic fragments in axon guidance. *J. Neurosci.*, **21**, 4281-4289.

Ott, H., Diekmann, H., Stuermer, C. A., and Bastmeyer, M. (2001). Function of Neurolin (DM-GRASP/SC-1) in guidance of motor axons during zebrafish development. *Dev. Biol.*, **235**, 86-97.

Pakkenberg, B. and Gundersen, H. J. G. (1997). Neocortical neuron number in humans: effect of sex and age. *J. Comp. Neurol.*, **384**, 312-320.

Park, K. W., Morrison, C. M., Sorensen, L. K., Jones, C. A., Rao, Y., Chien, C.-B., Wu, J. Y., Urness, L. D., and Li, D. Y. (2003). Robo4 is a vascular-specific receptor that inhibits endothelial migration. *Dev. Biol.*, **261**, 251-267.

Piper, M., Anderson, R., Dwivedy, A., Weinl, C., van Horck, F., Leung, K. M., Cogill, E., and Holt, C. (2006). Signaling mechanisms underlying Slit2-induced collapse of xenopus retinal growth cones. *Neuron*, **49**, 215-228.

Pittman, A. J., Law, M.-Y., and Chien, C.-B. (2008). Pathfinding in a large vertebrate axon tract: isotypic interactions guide retinotectal axons at multiple choice points. *Development*, **135**, 2865-2871.

Plachez, C., Andrews, W., Liapi, A., Knoell, B., Drescher, U., Mankoo, B., Zhe, L., Mambetisaeva, E., Annan, A., Bannister, L., Pamavelas, J. G., Richards, L. J. (2008). Robos are required for the correct targeting of retinal ganglion cell axons in the visual pathway of the brain. *Mol. Cell. Neurosci.*, **37**, 719-730.

Plump, A. S., Erskine, L., Sabatier, C., Brose, K., Epstein, C. J., Goodman, C. S., Mason, C. A., and Tessier-Lavigne, M. (2002). Slit1 and Slit2 cooperate to prevent premature midline crossing of retinal axons in the mouse visual system. *Neuron*, **33**, 219-232.

Pratt, T., Conway, C. D., Tian, N. M., Price, D. J., and Mason, J. O. (2006). Heparan sulphation patterns generated by specific heparan sulfotransferase enzymes direct distinct aspects of retinal axon guidance at the optic chiasm. *J. Neurosci.*, **26**, 6911 -6923.

Rajagopalan, S., Nicolas, E., Vivancos, V., Berger, J., and Dickson, B. J. (2000). Crossing the midline: roles and regulation of Robo receptors. *Neuron*, **28**, 767-777.

Rajagopalan, S., Vivancos, V., Nicolas, E., and Dickson, B. J. (2000). Selecting a longitudinal pathway: Robo receptors specify the lateral position of axons in the Drosophila CNS. *Cell*, **103**, 1033-1045.

Raper, J. and Mason, C. (2010). Cellular strategies of axonal pathfinding. *Cold Spring Harb. Perspect. Biol.*, **2**, a001933.

Renier, N., Schonewille, M., Giraudet, F., Badura, A., Tessier-Lavigne, M., Avan, P., De Zeeuw, C. I., and Chédotal, A. (2010). Genetic dissection of the function of hindbrain axonal commissures. *PLoS Biol.*, **8**, e1000325.

Rhee, J., Buchan, T., Zukerberg, L., Lilien, J., and Balsamo, J. (2007). Cables links Robo-bound Abl kinase to N-cadherin-bound [beta]-catenin to mediate Slit-induced modulation of adhesion and transcription. *Nat. Cell Biol.*, **9**, 883-892.

Rhee, J., Mahfooz, N. S., Arregui, C., Lilien, J., Balsamo, J., and VanBerkum, M. F. A. (2002). Activation of the repulsive receptor Roundabout inhibits N-cadherin-mediated cell adhesion. *Nat. Cell Biol.*, **4**, 798-805.

Ringstedt, T., Braisted, J. E., Brose, K., Kidd, T., Goodman, C., Tessier-Lavigne, M., and O'Leary, D. D. (2000). Slit inhibition of retinal axon growth and its role in retinal axon pathfinding and innervation patterns in the diencephalon. *J. Neurosci.*, **20**, 4983-4991.

Sabatier, C., Plump, A. S., Le M., Brose, K., Tamada, A., Murakami, F., Lee, E. Y., and Tessier-Lavigne, M. (2004). The divergent Robo family protein rig-1/Robo3 is a negative regulator of slit responsiveness required for midline crossing by commissural axons. *Cell*, **117**, 157-169.

Sakai, J. A. and Halloran, M. C. (2006). Semaphorin 3d guides laterality of retinal ganglion cell projections in zebrafish. *Development*, **133**, 1035-1044.

Seeger, M., Tear, G., Ferres-Marco, D., and Goodman, C. S. (1993). Mutations affecting growth cone guidance in Drosophila: genes necessary for guidance toward or away from the midline. *Neuron*, **10**, 409-426.

Shewan, D., Dwivedy, A., Anderson, R., and Holt, C. E. (2002). Age-related changes underlie switch in netrin-1 responsiveness as growth cones advance along visual pathway. *Nat. Neurosci.*, **5**, 955-962.

Simpson, J. H., Kidd, T., Bland, K. S., and Goodman, C. S. (2000). Short-range and long-range guidance by Slit and its Robo receptors: Robo and Robo2 play distinct roles in midline guidance. *Neuron*, **28**, 753-766.

Sperry, R. W. (1963). Chemoaffinity in the orderly growth of nerve fiber patterns and connections. *Proc. Natl. Acad. Sci. U.S.A.*, **50**, 703-710.

Spitzweck, B., Brankatschk, M., and Dickson, B. J. (2010). Distinct protein domains and expression patterns confer divergent axon guidance functions for Drosophila Robo receptors. *Cell*, **140**, 409-420.

Sretavan, D. W. (1990). Specific routing of retinal ganglion cell axons at the mammalian optic chiasm during embryonic development. *J. Neurosci.*, **10**, 1995-2007.

Steigemann, P., Molitor, A., Fellert, S., Jäckle, H., and Vorbrüggen, G. (2004). Heparan sulfate proteoglycan syndecan promotes axonal and myotube guidance by slit/robo signaling. *Curr. Biol.*, **14**, 225-230.

Stoeckli, E. T. and Landmesser, L. T. (1995). Axonin-1, Nr-CAM, and Ng-CAM play different roles in the in vivo guidance of chick commissural neurons. *Neuron*, **14**, 1165-1179.

Suh, L. H., Oster, S. F., Soehrman, S. S., Grenningloh, G., and Sretavan, D. W. (2004). L1/Laminin modulation of growth cone response to EphB triggers growth pauses and regulates the microtubule destabilizing protein SCG10. *J. Neurosci.*, **24**, 1976-1986.

Tongiorgi, E., Bernhardt, R. R., and Schachner, M. (1995). Zebrafish neurons express two L1-related molecules during early axonogenesis. *J. Neurosci. Res.*, **42**, 547-561.

Trowe, T., Klostermann, S., Baier, H., Granato, M., Crawford, A. D., Grunewald, B., Hoffmann, H., Karlstrom, R. O., Meyer, S. U., Müller, B., Richter, S., Nusslein-Volhard, C., Bonhoeffer, F. (1996). Mutations disrupting the ordering and topographic mapping of axons in the retinotectal projection of the zebrafish, Danio rerio. *Development*, **123**, 439-450.

Walz, A., McFarlane, S., Brickman, Y. G., Nurcombe, V., Bartlett, P. F., and Holt, C. E. (1997). Essential role of heparan sulfates in axon navigation and targeting in the developing visual system. *Development*, **124**, 2421 -2430.

Wang, K. H., Brose, K., Arnott, D., Kidd, T., Goodman, C. S., Henzel, W., and Tessier-Lavigne, M. (1999). Biochemical purification of a mammalian slit protein as a positive regulator of sensory axon elongation and branching. *Cell*, **96**, 771-784.

Weiner, J. A., Koo, S. J., Nicolas, S., Fraboulet, S., Pfaff, S. L., Pourquié, O., and Sanes, J. R. (2004). Axon fasciculation defects and retinal dysplasias in mice

lacking the immunoglobelseerfamily adhesion molecule BEN/ALCAM/SC1. *Mol. Cell. Neurosci.*, **27**, 59-69.

Williams, S. E., Mann, F., Erskine, L., Sakurai, T., Wei, S., Rossi, D. J., Gale, N. W., Holt, C. E., Mason, C. A., and Henkemeyer, M. (2003). Ephrin-B2 and EphB1 mediate retinal axon divergence at the optic chiasm. *Neuron*, **39**, 919-935.

Wilson, S. W., Ross, L. S., Parrett, T., and Easter, S. S., Jr (1990). The development of a simple scaffold of axon tracts in the brain of the embryonic zebrafish, Brachydanio rerio. *Development*, **108**, 121-145.

Wolman, M. A., Regnery, A. M., Becker, T., Becker, C. G., and Halloran, M. C. (2007). Semaphorin3D regulates axon axon interactions by modulating levels of L1 cell adhesion molecule. *J. Neurosci.*, **27**, 9653-9663.

Wong, K., Ren, X.-R., Huang, Y.-Z., Xie, Y., Liu, G., Saito, H., Tang, H., Wen, L., Brady-Kalnay, S. M., Mei, L., Wu, J. Y., Xiong, W. C., Rao, Y. (2001). Signal transduction in neuronal migration. *Cell*, **107**, 209-221.

Yu, T. W., Hao, J. C., Lim, W., Tessier-Lavigne, M., and Bargmann, C. I. (2002). Shared receptors in axon guidance: SAX-3/Robo signals via UNC-34/Enabled and a Netrin-independent UNC-40/DCC function. *Nat. Neurosci.*, **5**, 1147-1154.

Yuan, S. S., Cox, L. A., Dasika, G. K., and Lee, E. Y. (1999). Cloning and functional studies of a novel gene aberrantly expressed in RB-deficient embryos. *Dev. Biol.*, **207**, 62-75.

Yue, Y., Grossmann, B., Galetzka, D., Zechner, U., and Haaf, T. (2006). Isolation and differential expression of two isoforms of the ROBO2/Robo2 axon guidance receptor gene in humans and mice. *Genomics*, **88**, 772-778.

Zallen, J. A., Yi, B. A., and Bargmann, C. I. (1998). The conserved immunoglobulin superfamily member SAX-3/Robo directs multiple aspects of axon guidance in C. elegans. *Cell*, **92**, 217-227.

Zelina, P., Avci, H. X., Thelen, K., and Pollerberg, G. E. (2005). The cell adhesion molecule NrCAM is crucial for growth cone behaviour and pathfinding of retinal ganglion cell axons. *Development*, **132**, 3609-3618.

CHAPTER 2

PATHFINDING IN A LARGE VERTEBRATE AXON TRACT: ISOTYPIC INTERACTIONS GUIDE RETINOTECTAL AXONS AT MULTIPLE CHOICE POINTS

The following chapter is reprinted with permission from Pittman, A. J.*, Law, M.-Y.*, Chien, C.-B. (2008). Pathfinding in a large vertebrate tract: Isotypic interactions guide retinotectal axons at multiple choice points. *Development*, 135, 2865-2871.

*Authors contributed equally to the work.

Development ePress online publication date 23 July 2008

Development 135, 2865-2871 (2008) doi:10.1242/dev.025049

Pathfinding in a large vertebrate axon tract: isotypic interactions guide retinotectal axons at multiple choice points

Andrew J. Pittman[1,2,*], Mei-Yee Law[1,2,*] and Chi-Bin Chien[1,2,3,†]

Navigating axons respond to environmental guidance signals, but can also follow axons that have gone before – pioneer axons. Pioneers have been studied extensively in simple systems, but the role of axon-axon interactions remains largely unexplored in large vertebrate axon tracts, where cohorts of identical axons could potentially use isotypic interactions to guide each other through multiple choice points. Furthermore, the relative importance of axon-axon interactions compared with axon-autonomous receptor function has not been assessed. Here, we test the role of axon-axon interactions in retinotectal development, by devising a technique to selectively remove or replace early-born retinal ganglion cells (RGCs). We find that early RGCs are both necessary and sufficient for later axons to exit the eye. Furthermore, introducing misrouted axons by transplantation reveals that guidance from eye to tectum relies heavily on interactions between axons, including both pioneer-follower and community effects. We conclude that axon-axon interactions and ligand-receptor signaling have co-equal roles, cooperating to ensure the fidelity of axon guidance in developing vertebrate tracts.

KEY WORDS: Robo2, *astray*, *ath5*, *atoh7*, Morpholino, Fasciculation, Transplant, Cell-autonomy, Zebrafish

INTRODUCTION

To generate a functional nervous system, widely separated groups of neurons must form appropriate connections. Each newborn neuron extends an axon tipped by a motile growth cone, which navigates through sequential 'choice points' to eventually reach its target (Dickson, 2002; Guan and Rao, 2003; Tessier-Lavigne and Goodman, 1996). The growth cone has two potential sources of guidance information. First, it may fasciculate with 'pioneer' axons – defined here as earlier-born axons that share its path – using cell-adhesion molecules. Second, it may sense secreted or cell-surface guidance ligands produced by other cells in the brain, acting at long or short range, respectively. Most recent work has focused on guidance ligands; genetic screens and biochemical purification strategies have identified many ligand/receptor pairs used by navigating growth cones (Dickson, 2002; Guan and Rao, 2003; Tessier-Lavigne and Goodman, 1996).

There is long-standing evidence, however, that pioneer-follower interactions can play necessary roles in guidance (Lopresti et al., 1973; Bate, 1976; Raper et al., 1983; Raper et al., 1984; Kuwada, 1986; Klose and Bentley, 1989; Ghosh et al., 1990; Pike et al., 1992; Hidalgo and Brand, 1997; Jhaveri and Rodrigues, 2002; Williams and Shepherd, 2002). In other cases, pioneers are not required (Keshishian and Bentley, 1983; Holt, 1984; Eisen et al., 1989; Cornel and Holt, 1992) or only facilitate followers' guidance (Chitnis and Kuwada, 1991; Pike et al., 1992; Bak and Fraser, 2003). Nearly all of these studies were carried out in simple systems where a few pioneer axons could be identified, and where required roles for pioneers were tested by ablation. Furthermore, these pioneers were usually heterotypic: of a different neuronal type than the followers, with different origins and targets, so that they could only guide the followers through one leg of their journey. Thus, it is not clear (1) whether the role of pioneers is generalizable to more complex systems; (2) what the sufficient functions of pioneers are (for instance if they take abnormal paths); or (3) what roles are usually played by isotypic interactions (between axons from the same neuronal type).

In vertebrates, most axon tracts are built on a large scale. They typically comprise thousands of axons, all with the same origin and target, and often develop over an extended period as new neurons are added. This raises the possibility that vertebrate axons could be guided by isotypic interactions, either between earlier and later axons (pioneer-follower interactions), or between axons that grow at the same time (community interactions). As axons in the same tract share both origin and target, isotypic interactions could act at multiple choice points throughout their pathway. Although there is often an unspoken assumption that vertebrate axons indeed use pioneers for guidance, there have been only a few direct experimental tests of this hypothesis (Holt, 1984; Eisen et al., 1989; Ghosh et al., 1990; Cornel and Holt, 1992; Bak and Fraser, 2003). Here, we have used the zebrafish retinotectal system to study this fundamental cellular mechanism in axon guidance. We first ask whether isotypic pioneer-follower and community interactions are important in the development of a large vertebrate axon tract. We next use a pioneer replacement strategy to test whether pioneers are sufficient to affect followers, and to assess the relative importance of axon-axon interactions compared with guidance receptor signaling.

The retinotectal projection is one of the best-studied vertebrate tracts, the formation of which has been studied extensively (Erskine and Herrera, 2007). Retinal ganglion cell (RGC) axons must navigate out of the eye, across the optic chiasm, and dorsally through the optic tract to reach the optic tectum. Although retinal axons parallel the tract of the postoptic commissure (tPOC) after crossing the optic chiasm,

[1]Program in Neuroscience, University of Utah Medical Center, 20 North 1900 East, Salt Lake City, UT 84132, USA. [2]Department of Neurobiology and Anatomy, University of Utah Medical Center, 20 North 1900 East, Salt Lake City, UT 84132, USA. [3]Brain Institute, University of Utah Medical Center, 20 North 1900 East, Salt Lake City, UT 84132, USA.

*These authors contributed equally to this work
†Author for correspondence (e-mail: chi-bin.chien@neuro.utah.edu)

Accepted 25 June 2008

they make at most fleeting contacts with tPOC axons (Burrill and Easter, 1995), and embryological manipulations that remove tPOC axons do not affect retinal axon guidance (Cornel and Holt, 1992). Thus, retinal axons do not require heterotypic pioneers. Despite the extensive retinotectal literature, there has been only one functional test of whether retinal pioneer axons might guide later retinal axons (i.e. through an isotypic interaction). In *Xenopus*, dorsocentral RGCs are the first to send out their axons. There was no effect on the guidance of later retinal axons when heterochronic transplants were used to delay the outgrowth of dorsocentral RGCs (Holt, 1984), suggesting that retinal pioneers are not required. Here, we re-examine the role of retinal pioneers in guidance both within the eye and after exiting it. We use genetic and embryological manipulations both to remove early RGCs, and to replace them with cells that lack the Robo2 guidance receptor. We find that isotypic pioneers in fact play multiple roles during the formation of this archetypal vertebrate tract.

MATERIALS AND METHODS

Transgenics

All zebrafish were of the Tü or TL strains. The transgenic lines and mutant alleles used were: *Tg(isl2b:GFP)*^{zc7}, *Tg(isl2b:mCherry-CAAX)*^{zc23} or *Tg(isl2b:mCherry-CAAX)*^{zc25} (both of similar brightness), *Tg(brn3c:gap43-GFP)*^{s356t} (Xiao et al., 2005), and the null *ast* allele *ast*^{ti272z} (Fricke et al., 2001). As *ast* is homozygous adult viable, *ast* embryos were generated by incrossing homozygote parents. Embryos were raised at 28.5°C in 0.1 mM phenylthiourea and staged according to time postfertilization and morphology (Kimmel et al., 1995). Experimental procedures followed NIH guidelines and were approved by the University of Utah Institutional Animal Care and Use Committee.

Morpholino injections

Lyophilized *ath5*MO (5′-TTCATGGCTCTTCAAAAAAGTCTCC-3′, antisense start codon underlined; Open Biosystems/Gene Tools) was solubilized in 1× Danieau's buffer and aliquotted at –20ºC. Embryos from either *isl2b:GFP*/+ or *isl2b:mCherry-CAAX*/+ incrosses were collected at the one-cell stage, and a nominal volume of 1 nl MO was pressure injected at the yolk/cell interface using a Picospritzer (Parker). MO was diluted to working concentrations with 0.1% Phenol Red as a marker dye, and the injected bolus measured using an eyepiece micrometer. All embryos for the dose-response experiments of Figs 1 and 2 were injected in the same session with a single pipette, counting pressure pulses to deliver different doses. Individual live embryos were repeatedly assayed for GFP expression in the retina using a fluorescent dissecting microscope, every 3 hours from 33-57 hpf. Repeating this experiment yielded essentially the same results, except for a shift attributable to different bolus size (data not shown).

Cell transplants

Transplants were performed as described by Ho and Kane (1990). Briefly, one-cell donor embryos were injected with 5% rhodamine dextran (10,000 MW) as a lineage marker; at 4 hpf, 20-50 cells were transplanted to the animal pole of host embryos, which were raised to 5 dpf at 28.5°C. For Fig. 4, donors were from an *isl2b:mCherryCAAX*/+ incross, while hosts were *isl2b:GFP* embryos injected with 5 ng *ath5*MO.

In addition to RGCs, *isl2b:gfp* labels small clusters of neurons in the forebrain and dorsal diencephalon that make it difficult to unambiguously identify misrouted retinal axons. Therefore, axon-axon interaction experiments used the *Tg(brn3c:gap43-GFP)*^{s356t} transgene, which labels a subpopulation of ~50% of RGCs without confounding brain expression (Xiao et al., 2005). For Fig. 5, donors were from a *brn3c:GFP*/+ or *ast; brn3c:GFP*/+ incross, whereas hosts were wild type or *ast*. For Fig. 6, donors were nontransgenic, while hosts were *brn3c:GFP* embryos injected with 5 ng *ath5*MO.

Immunofluorescence and staining

For whole-mount immunostaining, *isl2b:GFP*-positive larvae were fixed at 5 or 6 dpf in 4% paraformaldehyde (PFA) in PBS overnight at 4°C, washed in PBST (PBS with 0.1% Tween-20), dehydrated through a methanol series, stored at –20°C for over 12 hours, rehydrated, washed in PBST, permeabilized with 0.1% collagenase for 1 hour at room temperature, then incubated in the following primary antibodies overnight at 4°C: rabbit anti-GFP (1:400; Invitrogen A11122), mouse anti-GFP (1:200; Chemicon MAB3580), rabbit anti-DsRed (1:200; Clontech 632496), mouse anti-parvalbumin (1:400; Chemicon MAB1572) or affinity-purified rabbit anti-Pax2a (1:300; gift of A. Picker). Larvae were then washed in PBST, incubated in goat anti-rabbit Alexa 488 (1:200; Invitrogen A11008), goat anti-mouse Cy3 (1:200; Jackson ImmunoResearch 115-165-003), goat anti-mouse Alexa 488 (1:200; Molecular Probes A-11029) or goat anti-rabbit Cy3 (1:200; Jackson ImmunoResearch 111-165-003), then stained in Hoechst 33342 (1:15,000; Molecular Probes H-3570) or ToPro-3 (1:1000; Molecular Probes T3605) for 30 minutes at room temperature. Whole-mount in situ hybridization for *netrin1a* was performed as described previously (Wilson et al., 2006). For sectioning, embryos were dehydrated in methanol, infiltrated at 4°C in 1:1 Immuno-Bed:methanol for 30 minutes then 100% Immuno-Bed overnight, oriented and embedded in 20:1 Immuno-Bed:Immuno-Bed Solution B (EMS 14260-04), and sectioned at 8 μm on a Reichert-Jung 2050 Supercut microtome with a glass knife.

Fluorescent microscopy

GFP expression was initially assayed using an Olympus SZX-12 fluorescent dissecting microscope with a 1.6× objective. For more detailed analysis of GFP expression and the retinotectal projection, live 5 dpf larvae were mounted in 1.5% low-melt agarose with tricaine and imaged with an Olympus confocal microscope. Images were processed using Adobe Photoshop CS2. The relatively small number of GFP+ axons in cell transplant experiments are obscured by skin autofluorescence when viewed as confocal projections. Therefore, for Figs 5 and 6, we used ImageJ (http://rsb.info.nih.gov/ij; developed by Wayne Rasband, NIH) and Photoshop to manually edit each *z*-slice and remove autofluorescence and background fluorescence, taking care always to spare nearby axons (see Fig. S3 in the supplementary material). Raw confocal stack data is available upon request. For cell counting, 42 hpf *isl2b:gfp* eyes were fixed, labeled with ToPro-3, dissected, mounted in 80% glycerol and imaged with an Olympus confocal microscope. ToPro3+, GFP+ nuclei were counted by manual inspection of each *z*-slice in the stack, and movies were made with Volocity software.

Phenotype quantification

In *ast*, eight retinal pathfinding errors are commonly seen: midline crossing in the habenular and posterior commissures, and left- and right-sided projections to the telencephalon, diencephalon and ventral hindbrain (see Fig. S2 in the supplementary material). For each chimeric larva, the presence (one or more axons) or absence of each error was scored at 5-6 dpf by an observer blinded to genotypes, using ImageJ to examine the entire (unedited) confocal *z*-stack. Scores were compared by the Mann-Whitney U test using Instat 3 (GraphPad).

RESULTS

To test the role of pioneer neurons, we devised a method to selectively remove early-born RGCs. These cells' differentiation starts ventroanteriorly at 27-28 hours postfertilization (hpf), spreading circumferentially to fill the central retina by ~40 hpf (Hu and Easter, 1999; Masai et al., 2005). After this, new RGCs are added in successive peripheral rings (Fig. 1A). The RGC-specific transgene Tg(*isl2b:GFP*)^{zc7} turns on by 30 hpf in ventroanterior retina, reliably labeling all or the vast majority of RGCs (Fig. 1B; A.J.P. and C.-B.C., unpublished). To remove early RGCs, we used a translation-blocking antisense morpholino oligonucleotide (*ath5*MO) to knock down function of *ath5* (*atoh7* – Zebrafish Information Network), a bHLH transcription factor expressed specifically in the eye and required cell-autonomously for RGC differentiation (Kay et al., 2005). *ath5* mutants completely lack RGCs (Brown et al., 2001; Kay et al., 2001), and their RGC progenitors seem instead to take on primarily bipolar cell fates (Kay

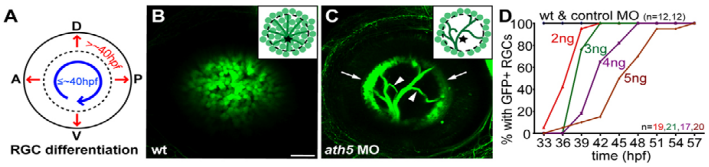

Fig. 1. *ath5* MO blocks differentiation of early- but not late-born RGCs. (**A**) Normally, early RGCs differentiate in a wave across central retina (blue arrow); late RGCs are then added centrifugally (red arrows). (**B,C**) 6 dpf *isl2b:GFP*, lateral views, anterior towards the left. Insets schematize cell bodies, axons and optic nerve head (star). (B) Wild-type eye shows GFP+ RGCs throughout central retina; axons are obscured by cell bodies. (C) A high dose of *ath5*MO blocks differentiation of early RGCs, but late RGCs still form (arrows). Without central RGCs, peripheral axons are visible (arrowheads). (**D**) Dose-response curve showing timing of RGC formation with different doses of *ath5*MO. In wild type and with 3 ng control MO, GFP+ RGCs appear by 33 hpf. Increasing concentrations of *ath5*MO increasingly delay the appearance of the first RGCs. A, anterior; D, dorsal; P, posterior; V, ventral. Scale bar: 50 μm.

et al., 2001). We reasoned that *ath5*MO should have a similar, but transient, effect as the efficacy of morpholinos wanes as their concentration is diluted by embryonic growth (Nasevicius and Ekker, 2000). Indeed, we found that *ath5*MO causes a loss of early-born central RGCs, but allows later-born peripheral RGCs to differentiate (Fig. 1C). In *isl2b:GFP* embryos injected with high-dose (5 ng) *ath5*MO (Fig. 1C; Fig. 2E; see Fig. S1 in the supplementary material), RGCs were found exclusively in peripheral retina at 6 days postfertilization (dpf) – over 4 days after central RGCs normally form – showing that differentiation is prevented rather than merely delayed. We next injected an *ath5*MO dose series, monitoring RGC differentiation in live embryos from 33 to 57 hpf. In control embryos, GFP+ RGCs were always present by 33 hpf. With successively higher doses, the first RGCs appeared successively later, until with 5 ng *ath5*MO RGCs did not appear until 42 hpf or later in 90% of embryos (Fig. 1D). Thus, varying the dose of *ath5*MO controls the time at which the first RGCs differentiate.

We then tested whether removing early-born RGCs affects the pathfinding of later axons (Fig. 2). In uninjected controls, the retinotectal projection is mature at 5 dpf, with both optic tecta strongly innervated (Fig. 2B; n=12/12). However, when central RGCs were removed by injecting 5 ng *ath5*MO, axons of late-born RGCs failed to exit from the eye into the brain (Fig. 2C; n=19/20). We hypothesized that this failure might be related to the time of first RGC differentiation. Therefore, we injected *isl2b:GFP* embryos with 2-5 ng *ath5*MO (Fig. 1D), plotting retinal exit at 5 dpf against the time of first RGC differentiation (Fig. 2D). Axons projected from eye to tectum in 100% of control larvae (uninjected, n=12; 3 ng control MO, n=12) and in 83% (45/54) of those morphants (MO-injected embryos) whose first RGCs were born by 42 hpf. By contrast, axons exited the eye in only 5% (1/20) of morphants whose first RGCs were born after 42 hpf. Instead, axons from peripheral RGCs grew within the RGC layer of the eye without entering the intraretinal region of the optic nerve (Fig. 2E, see Movie 1 and Fig. S1 in the supplementary material). A physical barrier is not likely the cause: *ath5* morphants have normal retinal lamination, and the presumptive optic nerve can still be distinguished (see Fig. S1 in the supplementary material). To test for changes in the environment of the presumptive optic nerve, we stained for Pax2, which labels the surrounding primitive glia (Macdonald et al., 1997), and for *netrin1a*, a marker of the optic nerve and optic nerve head (Fig. 3). Both markers appeared normal in *ath5* morphants. Taken together, these results strongly suggest that an isotypic pioneer-follower interaction is required for the axons of later RGCs to exit the eye, and, further, that this interaction occurs during a critical period before 42 hpf.

We next tested whether this pioneer-follower interaction is sufficient as well as necessary, by resupplying RGCs to *ath5* morphants. We targeted the presumptive eye field in blastula-stage transplants from *isl2b:mCherry-CAAX* donors into *isl2b:GFP* hosts injected with high-dose *ath5*MO (Fig. 4A). As *ath5* acts cell-autonomously (Kay et al., 2005), we expected that donor (non-morphant) RGCs would differentiate without affecting host cells. Indeed, whereas host RGCs were still restricted to peripheral retina, donor RGCs were found in central retina, and usually sent axons out of the eye to the tectum (Fig. 4B,C). Of 32 eyes with mCherry+ donor axons reaching the tectum, 24 (75%) showed rescue of retinal exit, with GFP+ host axons reaching the tectum (Fig. 4B). Retinotectal topography appeared unaffected: donor axons from

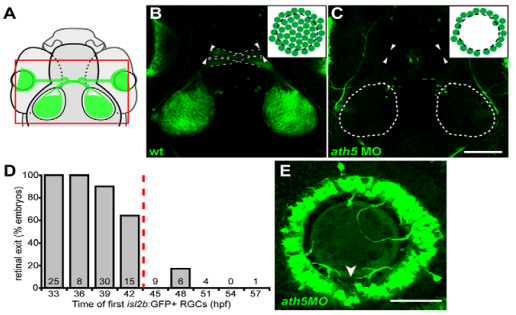

Fig. 2. Early RGCs are necessary for axons to exit eye. (**A**) Diagram showing field of view for B,C. (**B,C**) 5 dpf *isl2b:GFP*, confocal *z*-projections; dorsal views, anterior upwards. Insets show cell bodies in eye. (B) Wild-type axons exit eye (arrowheads), project through the optic chiasm (broken lines) and to the optic tecta. (C) With high dose of *ath5* MO, axons do not exit eyes (arrowheads) or innervate tecta (outlined). (**D**) Retinal exit in dose-response experiment of Fig. 1D, plotting percentage of embryos in which axons exit the eye against the time at which their first *isl2b:gfp*-positive RGCs were born. When RGCs are born by 42 hpf, axons usually exit the eye; when delayed after 42 hpf, axons rarely exit. Number of embryos is indicated at base of each bar. (**E**) 72 hpf *isl2b:GFP,* confocal *z*-projection; dorsal upwards. In a high-dose *ath5* morphant, axons from peripheral RGCs remain trapped in the RGC layer without entering the optic nerve. To better appreciate 3D structure, see volume reconstruction in Movie 1 in the supplementary material. Arrowhead indicates the optic nerve head, stained by anti-Pax2 (not shown). Scale bars: 100 μm in C; 50 μm in E.

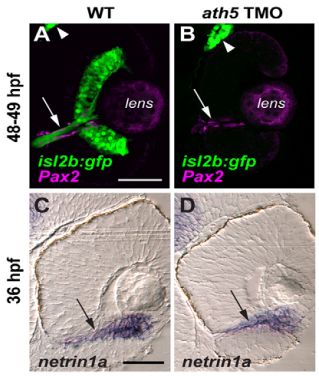

Fig. 3. *ath5* MO does not appear to affect the molecular and cellular environment of the optic nerve head or the intraretinal optic nerve. Coronal sections through 48-49 hpf *isl2b:GFP* (A,B) and 36 hpf non-transgenic (C,D) eyes, from either uninjected embryos (A,C) or embryos injected with high dose *ath5* TMO (B,D). (**A**,**B**) Pax2a antibody staining (magenta) labels presumptive glial cells which line the intraretinal region of the optic nerve (arrows) in both wild type (A) and *ath5* morphants (B). RGCs and their axons (green) are present in wild type (A), but not in *ath5* morphants (B). The trigeminal ganglion (arrowheads) is also labeled by *isl2b:gfp* and serves as a staining control. (**C**,**D**) In situ hybridization shows that *netrin1a* expression (arrows) surrounds the optic nerve and optic nerve head in wild type (C), and is unchanged in *ath5* morphants (D). Scale bars: 50 μm.

central retina projected to central tectum, and host axons from peripheral retina projected to peripheral tectum (Fig. 4B). Furthermore, imaging within chimeric eyes showed that late-born host axons appeared to fasciculate with donor axons (Fig. 4C-C″). Therefore, early RGCs are both necessary and sufficient to guide later axons out of the eye.

In a second series of experiments, we tested whether, after retinal axons exit the eye, interactions between them might affect guidance to the tectum. To do this, we used cell transplants to mix retinal axons of different intrinsic pathfinding potential. In *astray* (*ast*) mutants, retinal axons make drastic pathfinding errors because they lack the Slit receptor Robo2 (Fricke et al., 2001). Transplantation of eye primordia yields strictly eye-autonomous pathfinding defects, showing that Robo2 is required in the eye and not the brain (Fricke et al., 2001). Here, we performed cell transplants from WT or *ast* donors labeled with the RGC-specific transgene *brn3c:GFP* (Xiao et al., 2005) into nontransgenic wild-type or *ast* hosts (Fig. 5A). We then assayed the pathfinding of GFP-positive axons (which bear the donor genotype), quantitating the results by counting the number of classes of pathfinding errors made by GFP-positive donor retinal axons, yielding a score for each host from 0 for wild type to 8 for strong *ast* (see Fig. S2 in the supplementary material; see Materials and methods).

As expected, wild-type donor axons in wild-type hosts made no pathfinding errors (Fig. 5B,B′; 0.0±0.0 errors, mean±s.e.m.). Surprisingly, wild-type axons transplanted to *ast* hosts always made errors, which occurred at several different positions (Fig. 5C,C′; 2.71±0.40 errors, $P<0.0001$). Presumably, despite expressing functional Robo2, they were misguided by neighbors that lacked Robo2. Donor *ast* axons made many errors in *ast* hosts (Fig. 5D,D′; 7.93±0.07 errors), similar to axons in nontransplanted *ast* embryos (see Fig. S2 in the supplementary material). By contrast, *ast* axons transplanted into wild-type embryos navigated far better (Fig. 5E,E′; 2.86±0.31 errors, $P<0.0001$). Thus, even lacking functional Robo2, their pathfinding behavior was significantly rescued by wild-type neighbors. These effects are not transgene-dependent: using *isl2b:GFP* instead of *brn3c:GFP* yielded qualitatively similar results (data not shown). Strikingly, then, Robo2 acts nonautonomously in cell transplants, unlike its autonomous behavior in eye transplants (Fricke et al., 2001). As a receptor, the direct effects of Robo2 must take place in the growth cone that expresses it, but this does not mean that indirect effects cannot affect other axons. The strong effect of the genotype of the host axons on donor axon behavior shows that, despite the clear importance of Slit-Robo signaling, its role in individual axons can be overridden by axon-axon interactions.

Is this a pioneer-follower effect? As these chimerae contained far more host than donor cells, the host genotype could be affecting donor axon behavior because most pioneer axons are likely to be host derived. If so, replacing pioneer RGCs with cells of a different genotype should alter pathfinding by later axons. We tested this prediction by injecting high-dose *ath5*MO into *brn3c:GFP* hosts to remove all early RGCs, replacing the pioneer RGCs using transplants from nontransgenic donor embryos, then at 5 dpf assaying the pathfinding of GFP-positive axons, which are host-derived and therefore ‘follower’ axons (Fig. 6A). Wild-type

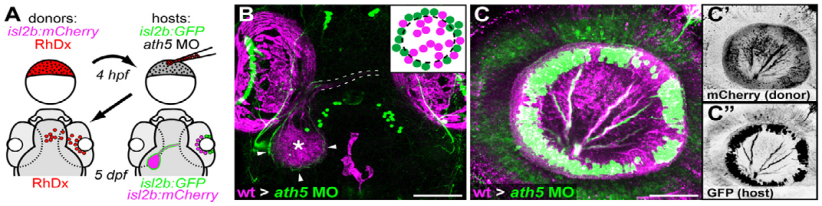

Fig. 4. Transplanted WT central RGCs rescue retinal exit in *ath5* morphants. (**A**) Blastula transplants from *isl2b:mCherry* donors resupply *ath5* morphant hosts, labeled with *isl2b:gfp*, with early RGCs. *RhDx,* rhodamine-dextran cell lineage marker. (**B**) Resupplied WT RGCs and axons (magenta) are sufficient to rescue host axons in morphants (green). Pigment cell autofluorescence is seen around eyes and at dorsal midline (magenta). Retinal axons project across chiasm (broken lines); donor axons terminate in central tectum (asterisk), while host axons terminate in peripheral tectum (arrowheads). Dorsal view, 5 dpf. (**C**) Lateral view of 5 dpf eye showing peripheral host axons (green) fasciculating with resupplied WT axons (magenta). (**C′**) Donor and (**C″**) host axons, reverse contrast. Scale bars: 100 μm in B; 50 μm in C.

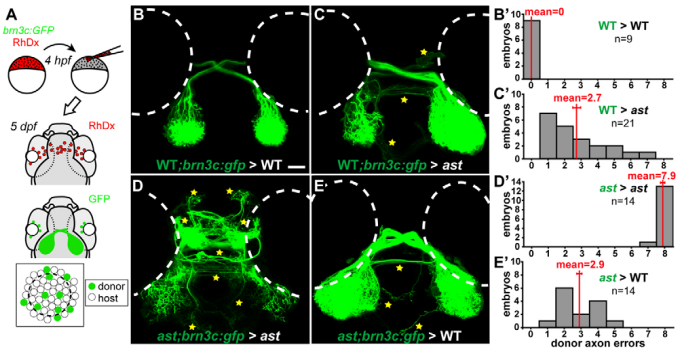

Fig. 5. Axon-axon interactions strongly influence retinotectal pathfinding. (**A**) Transplants yield GFP-expressing donor RGCs in host eyes. (B-E) Dorsal views, 5 dpf, rostral upwards. Donor axons labeled with *brn3c:GFP*; pathfinding errors indicated by yellow stars. (B′-E′) Error quantitation. (**B**,**B′**) In wild-type> wild-type transplants, donor axons pathfind perfectly. (**C**,**C′**) By contrast, when transplanted into *ast* hosts, wild-type axons make significantly more errors. (**D**,**D′**) As expected, *ast* donor axons make many errors in *ast* hosts. (**E**,**E′**) However, when transplanted into wild-type hosts, *ast* axons make significantly fewer errors. Scale bar: 50 μm.

followers made no errors when transplanted pioneers were wild type (Fig. 6B,B′; 0.0±0.0 errors). However, when pioneers were replaced with *ast* cells, wild-type followers made more errors (Fig. 6C,C′; 1.72±0.31 errors, $P<0.002$). Thus, misguided pioneers indeed influence wild-type followers. As expected, *ast* followers made many errors when pioneers were *ast* (Fig. 6D,D′; 5.96±0.33 errors). When pioneers were replaced with wild-type cells, *ast* follower axons made fewer errors (Fig. 6E,E′; 4.79±0.24 errors, $P<0.01$). Thus, the pathfinding of follower axons is partially influenced by the genotype of the pioneers, although clearly the genotype of the followers remains the predominant influence.

DISCUSSION

We have shown that early-born RGCs are both necessary and sufficient for retinal axons to exit the eye. This is a somewhat surprising result in light of an elegant study in *Xenopus* (Holt, 1984), which did not find an important role for retinal pioneers. We believe the difference derives from our ability to use *ath5*MO injection to completely prevent the development of all central RGCs. By contrast, the heterochronic transplants used in the *Xenopus* study only affected the dorsal half of central retina (the source of pioneers in *Xenopus*), and furthermore only delayed the development of retinal pioneers by 9-20 hours, rather than removing them entirely. A previous study in zebrafish had proposed that a small group (<10) of early retinal growth cones were pioneers based on their significant separation from the next growth cones to follow (Stuermer, 1988). It is clear from our *ath5* morpholino injections that these few growth cones are not functionally pioneers, in the sense of being necessary for the guidance of later axons. Instead, we find that far more cells must be removed to prevent retinal exit: the RGCs born by 42 hpf, the critical stage (Fig. 1), number about 600 (see Movies 2 and 3 in the supplementary material). This is strikingly different from invertebrate systems where ablation of a few pioneers is sufficient to perturb follower axons.

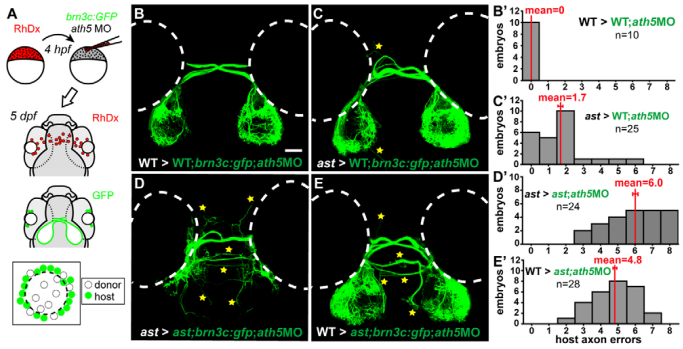

Fig. 6. Pioneer axons influence pathfinding of follower axons. (**A**) Transplants resupply early RGCs to *brn3c:GFP* hosts injected with *ath5* MO. (B-E) Dorsal views at 5 dpf, rostral upwards. Host axons terminate peripherally on the tectum; errors indicated by stars. (B′-E′) Error quantitation. (**B,B′**) In wild type>wild type;*ath5* MO transplants, host follower axons pathfind normally. (**C,C′**) When pioneers are replaced with *ast* cells, wild type follower axons make significantly more mistakes. (**D,D′**) In *ast*>*ast;ath5*MO transplants, host follower axons make many errors. (**E,E′**) When pioneers are replaced with wild-type cells, follower *ast* axons make fewer errors but are not completely rescued. Scale bar: 50 μm.

After retinal exit, our transplant experiments show that isotypic interactions between retinal axons are important for three further choice points that require Robo2 function (Fricke et al., 2001; Hutson and Chien, 2002) (M. Hardy and C.-B.C., unpublished). Misrouting in the optic chiasm leads to chiasm defasciculation (Fig. 6C); misrouting in the ventral optic tract leads to telencephalic or ventral hindbrain projections (Fig. 5C; Fig. 6C); and misrouting in the dorsal optic tract leads to aberrant crossing in the habenular or posterior commissures (Fig. 5C). At all three choice points, mutant axons can lead wild-type neighbors into error. Thus, axon-axon interactions function throughout the entire course of the retinotectal projection.

Several questions remain for future studies on axon-axon interactions. What distinguishes pioneers from followers? We know of no molecular markers that distinguish these RGC populations – for instance, they both express *robo2* (Campbell et al., 2007) – so the only difference may be the time and position of their birth. How do pioneers interact with followers within the eye? Most simply, later axons may fasciculate with early axons, as seen in Fig. 4C-C″; future experiments will test whether disrupting cell-adhesion molecules leads to axon guidance errors within the retina, as in other vertebrates (Brittis et al., 1995; Leppert et al., 1999; Ott et al., 1998; Zelina et al., 2005). However, we cannot formally exclude other possibilities. For example, early RGC cell bodies might secrete an attractant that draws later axons to the optic nerve head. Interestingly, WT>*ath5* morphant transplants in which host axons remained trapped within the eye tended to have fewer donor axons on the tectum (data not shown), presumably reflecting fewer donor RGCs, which might provide an insufficient level of attraction. What underlies the apparent crucial period before 42 hpf? Both timing and spacing are possible explanations. Ligands implicated in retinal exit (Birgbauer et al., 2000; Deiner et al., 1997; Kay et al., 2005; Kolpak et al., 2005; Li et al., 2005; Thompson et al., 2006) or their receptors, might be expressed only transiently during this period, so that RGCs born after 42 hpf would lack appropriate exit signals. Alternatively, early-born RGCs may be close enough to find the optic nerve head, whereas later-born RGCs are simply too far away to sense it.

Although most pioneer experiments have studied heterotypic axon interactions, there have been a few studies of isotypic interactions. In grasshopper, Myers and Bastiani (Myers and Bastiani, 1993) found that the growth cone of the identified Q1 neuron interacts strongly with its contralateral homolog, and that ablation of one Q1 often leads to midline stalling of the growth cone of the other Q1. In the zebrafish, Bak and Fraser (Bak and Fraser, 2003) found that pioneer and follower growth cones in the postoptic commissure (POC) display characteristic morphology and kinetics (spread/slow and narrow/fast, respectively). After laser ablation of pioneer growth cones, followers appeared to take their place and behave like pioneers. However, POC pioneer ablation did not have any effect on the pathfinding of follower axons, and indeed we do not know of previous studies in vertebrates showing guidance by isotypic pioneers.

Here, we found that isotypic interactions after retinal exit help to guide retinal axons to the tectum. We were able to test the role of axon-axon interactions in a new way: by replacing rather than ablating RGCs, we tested sufficiency rather than necessity. Previous studies on pioneers found that their ablation prevents normal pathfinding by followers (e.g. Raper et al., 1983; Klose and Bentley, 1989; Pike et al., 1992; Whitlock and Westerfield, 1998); here, we used zebrafish transplants to test how misrouted mutant axons affect wild-type axons, and vice versa. We found that *ast* host axons can misroute wild-type donor axons, whereas wild-type host axons rescue *ast* donors to a large degree. This allowed us to compare the relative importance of different guidance mechanisms; we conclude that axon-axon interactions can be just as important as cell-autonomous Slit-Robo signaling. As well as showing a significant role for pioneer-follower interactions, our data suggest an even more important role for peer interactions between late retinal axons. An *ast* host axon in a WT>*ast;ath5*MO transplant (Fig. 6E,E′) misroutes more often than an *ast* donor axon in an *ast*>WT transplant (Fig. 5E,E′), perhaps because a larger fraction of RGCs are *ast* in the former case. What might distinguish pioneer-follower from peer-peer interactions? We do not necessarily expect different molecular interactions but, instead, differences in temporal and spatial proximity. Peers grow out at the same time, whereas peripheral followers grow out significantly later than pioneers. New retinal axons grow at the surface of the brain, so that pioneers are gradually buried underneath. Thus, although peers can interact directly, late followers will contact pioneers only indirectly, with several degrees of separation.

Our results are complemented by a recent study (Gosse et al., 2008), which showed that even a single RGC transplanted into *lakritz/ath5* mutant hosts can sometimes navigate successfully to the tectum. Successful cases of tectal innervation showed a bias for central RGCs; furthermore, axons of single RGCs transplanted to peripheral retina often remained trapped within the eye. Tectal innervation appeared to be a rare event, as a large number (~5000) of transplants had to be performed; in similar experiments, transplanting a few RGCs into *lakritz* or *ath5* morphants, we also find that axons rarely reach the tectum (A.J.P. and C.-B.C., unpublished). Overall, these data are consistent with our model that a large population of central RGCs are required for peripheral axons to exit the retina.

Our transplant paradigms create artificial situations in which axon-axon interactions are at war with ligand-receptor signals. For instance, a wild-type axon surrounded by *ast* axons may be shown the correct path by signals from the brain, but tugged off-course by its neighbors. During normal retinotectal development, by contrast, all axons are wild type. Not only does every axon recognize the correct path to its target, but so do all its predecessors and neighbors. Therefore, signals from both outside the tract (guidance ligands) and within (axon-axon interactions) should act in coordination to produce the highly stereotyped, precise formation of this vertebrate axon tract. As interaction (fasciculation) between isotypic axons is widely observed, we propose that this coordinated strategy is probably used throughout the development of complex vertebrate nervous systems.

Finally, we point out significant implications for the interpretation of mutant axon guidance phenotypes. For example, imagine a tract that uses two guidance receptors, A and B, to sense partially redundant sets of guidance signals. Suppose that in the absence of fasciculation, knockout of A would cause 30% of the axons to misroute, whereas knockout of B would cause 10% errors. As most axons still navigate correctly, axon-axon interactions might in fact reduce the A mutant phenotype to 10%, and the B mutant phenotype to undetectable levels. Thus, genetic redundancy may act not only at the level of single axons, but also at the level of entire tracts.

We thank members of the Chien laboratory for discussions, Jude Rosenthal for technical assistance, Michael Bastiani and Richard Dorsky for comments on the manuscript, Tong Xiao and Herwig Baier for the *brn3c:gfp* line, Alexander Picker for anti-Pax2, and Hideo Otsuna for help with cell counts and 3D visualization. This work was supported by grants from the NIH/NEI and the University of Utah Research Foundation to C.-B.C.

Supplementary material

Supplementary material for this article is available at http://dev.biologists.org/cgi/content/full/135/17/2865/DC1

References

Bak, M. and Fraser, S. E. (2003). Axon fasciculation and differences in midline kinetics between pioneer and follower axons within commissural fascicles. *Development* **130**, 4999-5008.

Bate, C. M. (1976). Pioneer neurones in an insect embryo. *Nature* **260**, 54-56.

Birgbauer, E., Cowan, C. A., Sretavan, D. W. and Henkemeyer, M. (2000). Kinase independent function of EphB receptors in retinal axon pathfinding to the optic disc from dorsal but not ventral retina. *Development* **127**, 1231-1241.

Brittis, P. A., Lemmon, V., Rutishauser, U. and Silver, J. (1995). Unique changes of ganglion cell growth cone behavior following cell adhesion molecule perturbations: a time-lapse study of the living retina. *Mol. Cell. Neurosci.* **6**, 433-449.

Brown, N. L., Patel, S., Brzezinski, J. and Glaser, T. (2001). Math5 is required for retinal ganglion cell and optic nerve formation. *Development* **128**, 2497-2508.

Burrill, J. D. and Easter, S. S., Jr (1995). The first retinal axons and their microenvironment in zebrafish: cryptic pioneers and the pretract. *J. Neurosci.* **15**, 2935-2947.

Campbell, D. S., Stringham, S. A., Timm, A., Xiao, T., Law, M. Y., Baier, H., Nonet, M. L. and Chien, C. B. (2007). Slit1a inhibits retinal ganglion cell arborization and synaptogenesis via Robo2-dependent and -independent pathways. *Neuron* **55**, 231-245.

Chitnis, A. B. and Kuwada, J. Y. (1991). Elimination of a brain tract increases errors in pathfinding by follower growth cones in the zebrafish embryo. *Neuron* **7**, 277-285.

Cornel, E. and Holt, C. (1992). Precocious pathfinding: retinal axons can navigate in an axonless brain. *Neuron* **9**, 1001-1011.

Deiner, M. S., Kennedy, T. E., Fazeli, A., Serafini, T., Tessier-Lavigne, M. and Sretavan, D. W. (1997). Netrin-1 and DCC mediate axon guidance locally at the optic disc: loss of function leads to optic nerve hypoplasia. *Neuron* **19**, 575-589.

Dickson, B. J. (2002). Molecular mechanisms of axon guidance. *Science* **298**, 1959-1964.

Eisen, J. S., Pike, S. H. and Debu, B. (1989). The growth cones of identified motoneurons in embryonic zebrafish select appropriate pathways in the absence of specific cellular interactions. *Neuron* **2**, 1097-1104.

Erskine, L. and Herrera, E. (2007). The retinal ganglion cell axon's journey: insights into molecular mechanisms of axon guidance. *Dev. Biol.* **308**, 1-14.

Fricke, C., Lee, J. S., Geiger-Rudolph, S., Bonhoeffer, F. and Chien, C. B. (2001). astray, a zebrafish roundabout homolog required for retinal axon guidance. *Science* **292**, 507-510.

Ghosh, A., Antonini, A., McConnell, S. K. and Shatz, C. J. (1990). Requirement for subplate neurons in the formation of thalamocortical connections. *Nature* **347**, 179-181.

Gosse, N. J., Nevin, L. M. and Baier, H. (2008). Retinotopic order in the absence of axon competition. *Nature* **452**, 892-895.

Guan, K. L. and Rao, Y. (2003). Signalling mechanisms mediating neuronal responses to guidance cues. *Nat. Rev. Neurosci.* **4**, 941-956.

Hidalgo, A. and Brand, A. H. (1997). Targeted neuronal ablation: the role of pioneer neurons in guidance and fasciculation in the CNS of Drosophila. *Development* **124**, 3253-3262.

Ho, R. K. and Kane, D. A. (1990). Cell-autonomous action of zebrafish spt-1 mutation in specific mesodermal precursors. *Nature* **348**, 728-730.

Holt, C. E. (1984). Does timing of axon outgrowth influence initial retinotectal topography in Xenopus? *J. Neurosci.* **4**, 1130-1152.

Hu, M. and Easter, S. S. (1999). Retinal neurogenesis: the formation of the initial central patch of postmitotic cells. *Dev. Biol.* **207**, 309-321.

Hutson, L. D. and Chien, C. B. (2002). *astray/robo2* is required for guidance and error correction in zebrafish retinal axons. *Neuron* **33**, 205-217.

Jhaveri, D. and Rodrigues, V. (2002). Sensory neurons of the Atonal lineage pioneer the formation of glomeruli within the adult Drosophila olfactory lobe. *Development* **129**, 1251-1260.

Kay, J. N., Finger-Baier, K. C., Roeser, T., Staub, W. and Baier, H. (2001). Retinal ganglion cell genesis requires lakritz, a zebrafish atonal homolog. *Neuron* **30**, 725-736.

Kay, J. N., Link, B. A. and Baier, H. (2005). Staggered cell-intrinsic timing of ath5 expression underlies the wave of ganglion cell neurogenesis in the zebrafish retina. *Development* **132**, 2573-2585.

Keshishian, H. and Bentley, D. (1983). Embryogenesis of peripheral nerve pathways in grasshopper legs. III. Development without pioneer neurons. *Dev. Biol.* **96**, 116-124.

Kimmel, C. B., Ballard, W. W., Kimmel, S. R., Ullmann, B. and Schilling, T. F. (1995). Stages of embryonic development of the zebrafish. *Dev. Dyn.* **203**, 253-310.

Klose, M. and Bentley, D. (1989). Transient pioneer neurons are essential for formation of an embryonic peripheral nerve. *Science* **245**, 982-984.

Kolpak, A., Zhang, J. and Bao, Z. Z. (2005). Sonic hedgehog has a dual effect on the growth of retinal ganglion axons depending on its concentration. *J. Neurosci.* **25**, 3432-4341.

Kuwada, J. Y. (1986). Cell recognition by neuronal growth cones in a simple vertebrate embryo. *Science* **233**, 740-746.

Leppert, C. A., Diekmann, H., Paul, C., Laessing, U., Marx, M., Bastmeyer, M. and Stuermer, C. A. (1999). Neurolin Ig domain 2 participates in retinal axon guidance and Ig domains 1 and 3 in fasciculation. *J. Cell Biol.* **144**, 339-349.

Li, Q., Shirabe, K., Thisse, C., Thisse, B., Okamoto, H., Masai, I. and Kuwada, J. Y. (2005). Chemokine signaling guides axons within the retina in zebrafish. *J. Neurosci.* **25**, 1711-1717.

Lopresti, V., Macagno, E. R. and Levinthal, C. (1973). Structure and development of neuronal connections in isogenic organisms: cellular interactions in the development of the optic lamina of Daphnia. *Proc. Natl. Acad. Sci. USA* **70**, 433-437.

Macdonald, R., Scholes, J., Strahle, U., Brennan, C., Holder, N., Brand, M. and Wilson, S. W. (1997). The Pax protein Noi is required for commissural axon pathway formation in the rostral forebrain. *Development* **124**, 2397-2408.

Masai, I., Yamaguchi, M., Tonou-Fujimori, N., Komori, A. and Okamoto, H. (2005). The hedgehog-PKA pathway regulates two distinct steps of the differentiation of retinal ganglion cells: the cell-cycle exit of retinoblasts and their neuronal maturation. *Development* **132**, 1539-1553.

Myers, P. Z. and Bastiani, M. J. (1993). Growth cone dynamics during the migration of an identified commissural growth cone. *J. Neurosci.* **13**, 127-143.

Nasevicius, A. and Ekker, S. C. (2000). Effective targeted gene 'knockdown' in zebrafish. *Nat. Genet.* **26**, 216-220.

Ott, H., Bastmeyer, M. and Stuermer, C. A. (1998). Neurolin, the goldfish homolog of DM-GRASP, is involved in retinal axon pathfinding to the optic disk. *J. Neurosci.* **18**, 3363-3372.

Pike, S. H., Melancon, E. F. and Eisen, J. S. (1992). Pathfinding by zebrafish motoneurons in the absence of normal pioneer axons. *Development* **114**, 825-831.

Raper, J. A., Bastiani, M. and Goodman, C. S. (1983). Pathfinding by neuronal growth cones in grasshopper embryos. II. Selective fasciculation onto specific axonal pathways. *J. Neurosci.* **3**, 31-41.

Raper, J. A., Bastiani, M. J. and Goodman, C. S. (1984). Pathfinding by neuronal growth cones in grasshopper embryos. IV. The effects of ablating the A and P axons upon the behavior of the G growth cone. *J. Neurosci.* **4**, 2329-2345.

Stuermer, C. A. (1988). Retinotopic organization of the developing retinotectal projection in the zebrafish embryo. *J. Neurosci.* **8**, 4513-4530.

Tessier-Lavigne, M. and Goodman, C. S. (1996). The molecular biology of axon guidance. *Science* **274**, 1123-1133.

Thompson, H., Camand, O., Barker, D. and Erskine, L. (2006). Slit proteins regulate distinct aspects of retinal ganglion cell axon guidance within dorsal and ventral retina. *J. Neurosci.* **26**, 8082-8091.

Whitlock, K. E. and Westerfield, M. (1998). A transient population of neurons pioneers the olfactory pathway in the zebrafish. *J. Neurosci.* **18**, 8919-8927.

Williams, D. W. and Shepherd, D. (2002). Persistent larval sensory neurones are required for the normal development of the adult sensory afferent projections in Drosophila. *Development* **129**, 617-624.

Wilson, B. D., Ii, M., Park, K. W., Suli, A., Sorensen, L. K., Larrieu-Lahargue, F., Urness, L. D., Suh, W., Asai, J., Kock, G. A. et al. (2006). Netrins promote developmental and therapeutic angiogenesis. *Science* **313**, 640-644.

Xiao, T., Roeser, T., Staub, W. and Baier, H. (2005). A GFP-based genetic screen reveals mutations that disrupt the architecture of the zebrafish retinotectal projection. *Development* **132**, 2955-2967.

Zelina, P., Avci, H. X., Thelen, K. and Pollerberg, G. E. (2005). The cell adhesion molecule NrCAM is crucial for growth cone behaviour and pathfinding of retinal ganglion cell axons. *Development* **132**, 3609-3618.

CHAPTER 3

EXPRESSION AND FUNCTION OF ROBO2 SPLICE VARIANTS DURING AXON GUIDANCE

Introduction

The Roundabout (Robo) transmembrane receptors, which belong to the immunoglobulin superfamily of cell adhesion molecules (IgCAMs), were initially identified in a *Drosophila* mutant screen for genes controlling axon guidance at the midline in the central nervous system (Kidd et al., 1998; Seeger et al., 1993). Robos bind primarily to their ligands—Slits—through their Ig1 and Ig2 domains (Liu et al., 2004), and trigger downstream modulation of cytoskeletal structures, thus controlling the growth cone behavior underlying axon navigation and guidance. There are four vertebrate Robos, Robo 1-4. The Robo1, Robo2, and Robo3 receptors have overlapping expression patterns in the zebrafish central nervous system during development (Lee et al., 2001), while Robo4 is predominantly expressed in zebrafish endothelial cells and the central nervous system (Park et al., 2003). These overlapping expression patterns and functional studies in various model organisms demonstrate conserved roles of Robo receptors in axon guidance, for instance during midline crossing, and in neuronal cell migration (Chédotal, 2007; Ypsilanti et al., 2010).

Similar to other IgCAMs, Robo 1-3 (but not Robo4) have been shown to have alternative splice forms. For instance, different signal peptide and 5' untranslated regions in Robo1 and DUTT1 (Deleted in U-twenty twenty) lead to variation in expression and function of these two Robo1 isoforms in developing and adult mouse embryos. Mature Robo1 is slightly longer than the DUTT1 isoform and appears to have a more restricted expression in adult mouse tissue, compared to DUTT1, which is expressed in various tissues at all stages examined (Clark et al., 2002). Robo3 was initially found to be alternatively spliced based on the predicted genomic structure of human Robo3 (Jen et al., 2004). Its differently spliced N-terminal isoforms were shown to have different binding properties for Slits (Camurri et al., 2005). The alternate C-terminal isoforms, Robo3.1 and Robo3.2, have opposing roles in midline crossing of mouse spinal commissural axons (Chen et al., 2008). Robo1 and Robo2 repel commissural axons and determine laterality of the axons at the midline. In precrossing axons, Robo3.1 facilitates midline crossing of commissural axons by decreasing the repulsive response induced in growth cones by Robo1 and Robo2. After crossing, Robo3.2 is required to restore repulsion in the growth cones to repel axons from the midline (Chen et al., 2008).

In zebrafish, four Robo receptors are present and only Robo2 is expressed in the retinal ganglion cells (RGCs) (Bedell et al., 2005; Lee et al., 2001; Park et al., 2003;). Robo2 in RGCs plays multiple essential roles in retinal axon intraretinal guidance (Thompson et al., 2009), axon extension, dendritic extension and branching (Hocking et al., 2010), guidance in the optic chiasm (Fricke et al., 2001), guidance in the optic tract (Hardy, Ph.D. dissertation), and axon arborization and stabilization on the tectum (Campbell et al., 2007). So far, two Robo2 splice forms have been reported in zebrafish:

robo2_tv1 [excluding the conserved alternative exon (CAE)] is expressed primarily in the brain and eye starting from 1 day postfertilization (dpf), while expression of *robo2_tv2* (including the CAE) is essentially undetectable until it increases significantly at midlarval stages (15 dpf) (Dalkic et al., 2006). However, no functional difference is known between these two splice variants. Given the many roles played by Robo2 in various stages of retinal axon elongation, the number of Robo2 splice variants may allow this single gene to fulfill multiple functions.

In this chapter, I describe three additional Robo2 splice isoforms present in young embryos and a specific role in axon guidance for one of them. I show that expression of exons 7, 19, and 23 in *robo2* is spatially (comparing eye to noneye tissue) and temporally regulated over the course of retinal axon elongation to the tectum. Taking advantage of the ability of morpholinos to inhibit specific splice variants, I uncover a novel function of exon 23 during early zebrafish development. Domains encoded by exon 23 are not required for RGC and primary commissural ascending neuron (CoPA) axon pathfinding during their initial outgrowth. However, they are necessary for correct axon targeting of olfactory receptor neurons (ORN) to the olfactory bulb.

Materials and methods

Fish stocks

Zebrafish were maintained according to standard procedures (Westerfield, 1995). Embryos were raised at 28.5ºC and staged based on timing and body morphology (Kimmel et al., 1995). Four different stable transgenic fish lines were used in this study: Tg(*isl2b:GFP*)^{zc7} (Pittman et al., 2008), Tg(*omp:YFP*) [official name Tg(*-6.0omp:gap43-*

YFP)^{rw031}] (Miyasaka et al., 2005), Tg(*isl2b:GFP*)^{zc7};*ast*^{ti272z}, and Tg(*brn3C:GFP*)^{s356t};*ast*^{zc10} [official name Tg(*pou4f3:gap43-gfp*)^{s356t};*ast*^{zc10}].

Isolating RNA for reverse transcription- and real-time PCR

Eyes were dissected in 100% MeOH and stored in 100% MeOH or RNAlater (Sigma) until RNA extraction. Dissected eyes, noneye tissue, and whole embryos were collected in separate microfuge tubes at 24, 36, 48, and 72 hours postfertilization (hpf), and 6 dpf. After embryos were anesthetized with tricaine, Trizol reagent (Invitrogen #15596) was added to the tube to homogenize the samples by triturating with hypodermic needles, then kept at -20 ºC until used. Total RNA was extracted using the RNeasy mini kit (Qiagen) following the manufacturer's protocol. DNaseI was used after total RNA extraction and before reverse transcription steps to eliminate genomic DNA.

In situ hybridization

A 1.5 kb partial *robo2* cDNA, 220 bp including exon 23, and 220 bp lacking exon 23 were amplified by direct PCR or fusion PCR from *robo2* plasmid, with T7 RNA polymerase promoter sequence incorporated into the antisense primer sequences. Primer sequences available upon request.

Digoxigenin (DIG)-labeled riboprobes were generated by in vitro transcription directly from PCR products. Whole-mount in situ hybridization was carried out according to Thisse and Thisse (2008). After stopping the color reaction with PBST washes, embryos were fixed with 4% paraformaldehyde for 20 minutes at room temperature, and cleared through a glycerol dilution series.

Immunohistochemistry

Whole-mount immunohistochemistry was performed as previously described (Pittman et al., 2008). Briefly, embryos were fixed with 4% paraformaldehyde overnight at 4ºC. After rinsing twice with PBST (PBS with 0.1% Tween-20), embryos were incubated in 0.1% collagenase to permeabilize, rinsed twice with PBST, and incubated in blocking solution (0.1%NCS/PBST) for 30 minutes. Rabbit anti-GFP primary antibody (Invitrogen) and Alexa-488 anti-rabbit secondary antibody (Invitrogen) were used at 1:200, overnight at 4ºC. Embryos were washed with PBST three times for 1 hour each after antibody incubations.

Morpholino injection

Antisense morpholino oligonucleotides (MOs) (Gene Tools, LLC) were resuspended in 1x Danieau buffer and mixed with 0.2% phenol red before injecting into one-cell stage embryos. To test the effective MO concentration to use, each MO was injected in increasing 2ng increments and efficacy analyzed by RT-PCR. MO sequences are as follows:

MO-7a (i6e7): 5'-GCGAGCTGAAGACACAACAATGGTA-3'

MO-7d (e7i7): 5'-ATAGAAGGATGGCTACTTACCAACA-3'

MO-19a (i18e19): 5'-GACTGAACTGCAAAAACAAGAAGAC-3'

MO-19d (e19i19): 5'-ACGGGACAAATGAACAGTACCTGCA-3'

MO-23a (i22e23): 5'-CTATAGTGGAGGCGAAGGGCAAAAA-3'

MO-23d (e23i23): 5'-GGACCAGTCCAATACCAACCTGACA-3'

MO-22a (i21e22): 5'-CATCACATCTGAAAGGCAGGAAAAG-3'

MO-22d (e22i22): 5'-TCAGATTGACTCACTGTTATTGCAG-3'

MO-25a: no good oligos could be designed

MO-25d (e25i25): 5'-TCTTTAAGTCAAATCTTACCAAGTC-3'

MO-29a (i28e29): 5'-ATCTGGAACAGAAGCGACAAGAGCC-3'

MO-29d (e29i29): 5'-GAATGAAACATTTTACCTGAAAAGG-3'

Results

Expression and function of alternatively spliced exons

Identification of *robo2* alternatively spliced exons

Only two zebrafish *robo2* isoforms have been reported so far, but no functional relevance has been identified. Dalkic et al. (2006) showed that the CAE (exon 27 in our analysis) is only present in zebrafish larvae that are at least 2 weeks old. Comparing genomic and transcript sequences from the Ensembl zv9 database (15:37845184-38213653) and the full-length *robo2* cDNA sequence we previously isolated (Lee et al., 2001), we found that the zebrafish *robo2* gene comprises at least 31 exons. Of these 31 exons, sequencing with cDNA obtained from 5 dpf embryos showed the presence of several splice variants (Figure 3.1), each of which is generated by the inclusion or skipping of an exon. The first alternately-employed 12-bp exon encodes Arg-Pro-Val-Ala between Ig domains 2 and 3. This short exon (exon 7) shares 100% amino acid identity with human and rat Robo2. The second exon of interest (exon 19) encodes an intracellular fragment adjacent to the transmembrane domain. The peptide encoded by this 27-bp exon shares 78% amino acid similarity with zebrafish Robo1 and 67% with zebrafish Robo3 but is not annotated for human, mouse, or rat Robo2. The third exon (exon 23) spans 126 bp in length and encodes a peptide lying between two conserved domains, CC1 and CC2, in vertebrates (Bashaw et al., 2000). This is a highly conserved

exon compared to human (97% amino acid similarity), and to mouse and rat (91%), in addition to sharing 37% amino acid similarity with zebrafish Robo1. The strikingly high conservation of exons 7 and 23 within vertebrates strongly suggests conserved functions of the domains encoded by these exons.

Alternative splicing of Robo2 exons is regulated during development

In order to investigate whether exons 7, 19, and 23 are differentially expressed in different tissues of developing zebrafish embryos, I compared expression in the eye versus the rest of the body across several important developmental time points, including just before RGC differentiation (24 hpf), during retinal axon guidance (36 hpf), as retinal axons reach the tectum (48 hpf), and during synaptic refinement (6 dpf). β-actin was used as a loading control. For example, exon 7 can be included (*robo2 ex7+*) or excluded (*robo2 ex7-*) in the transcripts. Inclusion of exon 7 in eye tissue is regulated during development (Figure 3.2A, B). *Robo2 ex7+* is detected at all stages of eye development and retinal axon elongation (24 – 48 hpf) (Figure 3.2A). However, *robo2 ex7-* is not present or expressed at a very low level in 24 hpf and 36 hpf eyes. Its expression increases at 48 hpf, but then strongly decreases by 6 dpf, when most retinal axons have reached the tectum and arborized in their target area. Similarly, *robo2 ex19-* and *robo2 ex23-* are expressed at very low levels in younger eyes, but their expression strongly increases in the retina after 36 hpf (Figure 3.2A, B). In contrast to the eye tissue, the collected body tissue expresses all forms, with and without the exons of interest, at all stages examined. These observations indicate that expression of *robo2* splice isoforms is not only temporally but also spatially regulated during development.

Splicing of robo2 exons is independently regulated

Spatial and temporal regulation of *robo2* exons 7, 19, and 23 can give rise to increased protein diversity. However, I wondered whether inclusion of these exons occurs concomitantly in the same transcript or is independently regulated. To test this, I carried out RT-PCR analysis that would assay multiple splice combinations in the developing embryos and compared expression in the eye and noneye tissue. Due to the distance of exon 7 from the other two alternatively spliced exons, 19 and 23, I was only able to examine whether exons 19 and 23 were present together in *robo2* transcripts.

ex19+ex23+ and *ex19- ex23+* are the predominant forms present in eye tissue at 24 hpf (Figure 3.2C). At 36 hpf and 48 hpf, when more RGCs have differentiated and some axons have crossed the midline, relative expression of the different transcripts in the eyes changed, with increased expression of *ex19+ ex23-* and *ex19-ex23-*. Interestingly, splice form expression patterns are further modified in more mature eyes at 6 dpf, where the predominant forms are *ex19+ ex23-* and *ex19-ex23-*, while transcripts including exon 23 are no longer detected. Thus, the expression of the different splice isoforms appears very dynamic over the course of eye maturation and retinal axon growth.

In noneye tissue, all four splice variants are present at all stages tested. *Ex19+ ex23+* and *ex19- ex23+* appear as the major transcripts present in the body, with *ex19+ ex23-* and *ex19- ex23-* being expressed at a much lower level. The ratio of the various splice forms expressed remains stable in noneye samples representing a heterogeneous collection of tissues (Figure 3.2C).

Loading for each amplification reaction was not normalized due to the technical difficulties of obtaining eye tissue in young embryos, so intensity cannot be compared across time points. Nonetheless, comparison of amplicons within an amplification reaction gives us information about regulation of splicing of exons 19 and 23. For instance, in the eye at 24 hpf, the expression levels of ex19+ and ex19- isoforms are very similar, whereas expression of ex23+ forms is much higher than that of ex23- forms. Analysis of the ex19+/- and ex23+/- levels over time reveals that splicing of these two exons is independently regulated.

Approach to test function of alternatively spliced exons

To test whether these alternatively spliced exons have specific functions during development, I used MOs to induce complete exon skipping. All the morpholino experiments were done in *isl2b:GFP*^{zc7} transgenics to aid visualization of retinal axons. Since morpholinos are known to have off target effects, I used two independent MOs, splice donor (MO-d) and splice acceptor (MO-a), to test the function of each exon unless no efficient morpholino targeting the sequence of the intron-exon boundaries could be designed (Table 3.1).

Among the three alternatively spliced exons tested, exon 7 is the shortest, only 12 bp in length. Even at high concentrations, both exon 7 MOs were toxic and failed to induce exon skipping. Therefore, the function of this particular exon could not be assessed. Exon 19 is mostly skipped with the highest concentration of MO-d. However, presumably due to toxicity effects induced by the MO, RGC differentiation is affected and delayed in the morphants. Development in other parts of the embryo is mostly normal, as evidenced by the differentiation of the trigeminal ganglion and its axonal

elongation (data not shown). Exon 19 MO-a does not give complete exon skipping at a toxic dose. Thus, the role of exon 19 in retinal axons could not be assessed. Exon 23 was effectively excluded after injecting with MO-a or MO-d. The phenotype observed in the morphants will be described in the next section.

Functions of *robo2* exon 23 during development

We designed two MOs which effectively induce complete skipping of exon 23. Despite the sequence conservation of exon 23 among vertebrates, no interacting partner or function of exon 23 has been attributed to its encoded domain. When injected with ex23MO-a, exon 23 is efficiently skipped (RT-PCR not shown). In situ hybridization with a long *robo2* RNA probe at 32 hpf shows staining in the olfactory placode, brain, and spinal cord (Figure 3.3A-B') as previously described (Lee et al., 2001). Exon 23 specific probes (Figure 3.3C-C') and exon 22/24 specific probes (Figure 3.3E-E') show staining similar to the long *robo2* probe. When exon 23 is skipped using our morpholino injection, staining with exon 23 specific probes is significantly decreased (Figure 3.3D, D'). In contrast, staining with ex22/24 probe is increased (Figure 3.3F, F'), showing that the MO is very effective in specifically inducing exon 23 skipping. All in situ conditions were kept constant, including colorimetric development. RT-PCR from control and morphant cDNA showed clean in-frame exon skipping with the morpholino after sequence analysis (data not shown).

The exon 23 loss-of-function analysis shows that domain encoded by the exon is not necessary for the role of Robo2 in retinal axon repulsion (data not shown). To test for a potential role of exon 23 in negatively regulating Robo2 axon repulsion activity, I injected the morpholino into a weak *astray* mutant, the *zc10* allele. The *zc10* allele was

discovered in a nonallelic noncomplementation screen for *robo2*. It has no mutation in its *robo2* coding sequence and no causative mutation has been identified (Ken Rasband, unpublished results). Eight common pathfinding errors are commonly seen in the strong *astray*^{ti272z} allele (Pittman et al., 2008). In each embryo, I counted the number of errors present. *zc10* scores an average of 3.7±0.3 (mean±S.E.M.) (Figure 3.4B, B') in an 8-point scoring system. Comparing to uninjected *zc10* embryos, morpholino injected *zc10* mutants have an average of 3.9±1.3 retinal axon pathfinding errors (Figure 3.4C, C'). The nearly identical number of pathfinding errors made in controls and morphants suggests that exon 23 does not play a positive or negative role in Robo2 function in retinal axon navigation.

In addition to RGC axon guidance errors, CoPA axons in the spinal cord are known to be affected in *robo2* mutants (Bonner and Dorsky, unpublished results). In wild-type, CoPA neurons in the dorsal spinal cord extend axons towards the floorplate, cross the midline, and are then presumably repelled by Slit expression at the floor plate and travel dorsally to the dorsal longitudinal fasciculus (DLF) (Figure 3.5A). CoPA axons in *ast*^{ti272z} mutants are thought to be insensitive to the Slit gradient from the floor plate, leading to a range of phenotypes: about half of the axons continue to stay close to the floor plate after crossing the midline; some gradually grow dorsally; and others have an axon trajectory that resembles the wild-type (Figure 3.5B, D). Unlike the zebrafish *ast*^{ti272z} null mutants, CoPA axons in exon 23 morphants appeared able to respond to Slits from the floor plate after crossing the midline (Figure 3.5D). Most of the axons follow a wildtype CoPA axon path, in which the axons quickly leave the floor plate upon midline

crossing. My results suggest that the domain encoded by exon 23 is not required in retinal axon and CoPA axon pathfinding.

In contrast, in preliminary experiments the ORN axons appear to be affected in exon 23 morphants (Figure 3.6). Similar to the loss of function phenotype in mouse and zebrafish *robo2* mutants, the ORN axons in the morphants were unable to form a tight bundle projecting towards their target in the olfactory bulb when exon 23 is skipped. Instead, ORN axons spread widely and wander aimlessly in the forebrain in 32.5 hpf zebrafish larvae (Figure 3.6B). However, this qualitative observation in exon 23 morphants needs to be confirmed with further experiments.

Functions of conserved domains

Conserved motifs in the Robo2 intracellular domain

In addition to functional tests for alternatively spliced exons, I used the same exon-skipping strategy to test the functions of other conserved exons, subject to a requirement that they be a multiple of 3 bp long. There are two Robo2 intracellular motifs, vCC1 and vCC2, conserved only within vertebrates but not to invertebrates. In addition to conservation with Robo2 in various species, these motifs are also conserved in other zebrafish Robos (Challa et al., 2001). It is not simple to test the role of the vCC1 domain with a morpholino due to the 122 bp length of exon 21, which encodes it (Figure 3.1). Deletion of this exon will presumably lead to a frameshift because its length is not a multiple of 3 bp. On the other hand, the 31-amino acid long vCC2 domain falls within the 264 bp exon 25, whose skipping will result in an in-frame deletion while the exon 25 splice acceptor sequence was not suitable for MO design. However, the exon 25 donor morpholino failed to cause exon skipping even at a high (toxic) dose. Thus it was not

possible to test whether the vCC1 and vCC2 domains are important in retinal axon guidance by using targeted morpholinos.

There are four *robo2* intracellular motifs conserved between vertebrates and invertebrates, namely CC0 – 3. CC0 and CC1 consist of eight or nine amino acids each, both falling within the 276 bp exon 22 sequence. I was able to attempt skipping of exon 22 because it is a multiple of 3 bp long (Table 3.1). Results with exon 22 will be further discussed in the next section. The CC2 motif is nine amino acids in length and rich in proline residues, suggesting structural and functional importance. However, since exon 24 is 160 bp long, I was not able to design a morpholino to test its required function. The CC3 motif is known to interact with several cytoskeletal-modifying molecules, such as Abl, srGAP1/3, and Dock/Nck. To skip exon 29, I tried both acceptor and donor MOs, but these proved ineffective for exon skipping with nontoxic doses.

Functional test of *robo2* exon 22

Embryos were deformed at low doses of MO-a; neither was there exon skipping at this toxic dose. Donor morpholinos targeted to the same exon did not result in exon skipping even at 20ng, which is quite high compared to many other morpholinos used. Interestingly, the morphants had a retinal axon pathfinding phenotype that was similar to *astray*^{ti272z} (null) mutants, but weaker. The phenotypes in the morphants could be classified into three categories: anterior projection, diencephalic projection, and single-tectum innervation (Figure 3.7). Individual morphants usually made only one type of pathfinding error, in contrast to *astray*^{ti272z} embryos which normally make an average of eight pathfinding errors (Pittman et al., 2008). The single-tectum phenotype seen in exon 22 morphants is also not found in *astray*^{ti272z} mutants. Sequencing of morphant cDNA

within regions close to exon 22 showed that the phenotype is probably due to an in-frame deletion of the vCC1 domain.

Discussion

In the first part of this chapter, I investigated the expression patterns of various *robo2* splice variants and their functions during axon navigation. All three alternatively spliced exons have lengths that are multiple of 3 bp, and are highly conserved between zebrafish and human. I found that expression patterns of these exons are spatially regulated between retina and nonretina (body) tissue at all time points examined. Within the retina, temporal regulation of the splice variants is especially obvious between 24 hpf and 36 hpf retina. These findings suggested that these splice forms may increase protein diversity and functions in the process of RGC navigation. However, it is not clear from expression pattern alone how splice forms correlate with functions at various choice points along the retinotectal pathway. This is further complicated by the fact that the three alternatively spliced exons may give rise to nine *robo2* splice variants. Limited by the technique of in situ hybridization, it is only possible for us to examine the localization of exon 23 at the mRNA level. Exon 7 and exon 19 are two short exons that do not allow design of specific probes with current methods. Robo2 protein expression of these different splice variants could help us to identify where and when the splice variants may have a role in retinotectal pathfinding. At present, there is no available Robo2 antibody that works in zebrafish wholemount staining. I have tried several commercially available Robo2 antibodies specific to human or mouse *robo2* sequences but to no avail. A previous graduate student in our lab tried to generate an antibody but failed. Also, I did not further test whether spatial regulation of various splice forms occurs between

different populations of nonretina tissue since this work was initially designed to study expression and functions of splice variants in the retina. It is possible that there will be spatial and temporal regulation elements among different tissues in the developing body.

I then investigated functional roles of these splice variants and conserved motifs (CC0 and CC1 in exon 22) using a loss-of-function method. Due to the limitations of morpholinos, only exon 23 and exon 22 can be tested with this method. Interestingly, human *robo2* exon sequence that corresponds to exon 23 in zebrafish *robo2* has also been found to be alternatively spliced (Yue et al., 2006). However, no functional roles are known for this exon. In this chapter, I described the timing and spatial regulation of various splice variants and carried out the first work to study the functions of Robo2 splice isoforms in axon pathfinding. Ex23MO-a effectively induces skipping of exon 23 but also causes nonspecific effect in delaying RGC differentiation in the retina. Since *astray*^{ti272z} null mutants do not show the same phenotype during development, it is highly likely that off-target morpholino effects cause the nonspecific phenotype in the retina. A method to test this hypothesis will be to inject the same morpholino (ex23MO-a) into *astray*^{ti272}. The experiment should confirm that the morpholino causes a nonspecific effect in the RGCs even in the absence of functional Robo2. In contrast, if RGC differentiation is only affected in *isl2b:GFP* but not in *astray*^{ti272} morphants, this shows that perhaps exon 23 has a new, unknown role in the early stages of normal RGC development. Rescue experiments to introduce different *robo2* deletion constructs into *astray*^{ti272} will be a useful alternative method to test exons or motifs in the Robo2 receptor. Another exon that I have tested, exon 22, yields surprising results, also due to morpholino side effects. The vCC1 conserved domain in the immediately upstream exon (exon 21) shows an

internal in-frame deletion in ex22MO-a morphants. However, more experiments, such as gain-of-function experiments in *astray*^{ti272}, are needed to confirm the function of exon 21 in interretinal axon guidance.

Morpholinos present a powerful tool for testing the required function of a gene or in this case, a specific exon, quickly and without going through the process and time of generating a stable transgenic line. Nonetheless, limitations including the infamous toxicity effects and off-target effects that can result with any morpholino cannot be overlooked. In addition, not all exons can be skipped without causing a frameshift due to the exon length. To circumvent these limitations, I tried to express Robo2 transiently with various promoters. I first tried the *islet-2b (isl2b*) promoter, which is commonly used in our lab to drive expression in RGCs, either as a direct fusion with GFP or using 2A peptide or IRES linker, but in this case it failed to overexpress *robo2*. The *isl2b-gata2* enhancer-promoter, in which the *isl2b* promoter has been replaced with the strong *gata2* basal promoter, also failed to induce visible *robo2* expression. In addition, *dlx*, *UAS*, and *CMV* promoters that are regularly used in other experiments also failed to drive detectable expression of *robo2* in both wildtype and *astray* embryos. I then tried using the *heat shock protein* (*hsp70l*) promoter, which is known to induce strong transcription activity when activated by higher temperature. Approximately 4 hours after heat shock, GFP signal from a direct fusion to Robo2 was visible—mainly in the muscles—but quickly disappeared about 14 hours post-heat-shock. Although intron sequences and 3'UTRs can help gene translation in some instances, *robo2* endogenous intron sequence (introns 11-13) and the beta-actin 3'UTR did not make *robo2* expression strong enough for analysis. Injecting *robo2* mRNA into wildtype embryos was effective only up to

1.5dpf and would not be sufficient for retinal axon analysis. In summary, I was not able to overexpress *robo2* in wildtype or *astray* embryos to carry out the next test to examine the function of specific domains of interest.

Reference

Bashaw, G. J., Kidd, T., Murray, D., Pawson, T., and Goodman, C. S. (2000). Repulsive axon guidance: Abelson and Enabled play opposing roles downstream of the roundabout receptor. *Cell*, **101**, 703-715.

Bedell, V. M., Yeo, S.-Y., Park, K. W., Chung, J., Seth, P., Shivalingappa, V., Zhao, J., Obara, T., Sukhatme, V. P., Drummond, I. A., Li, D. Y., Ramchandran, R. (2005). Roundabout4 is essential for angiogenesis in vivo. *Proc. Natl. Acad. Sci. U.S.A.*, **102**, 6373-6378.

Campbell, D. S., Stringham, S. A., Timm, A., Xiao, T., Law, M.-Y., Baier, H., Nonet, M. L., and Chien, C.-B. (2007). Slit1a inhibits retinal ganglion cell arborization and synaptogenesis via Robo2-dependent and -independent pathways. *Neuron*, **55**, 231-245.

Camurri, L., Mambetisaeva, E., Davies, D., Parnavelas, J., Sundaresan, V., and Andrews, W. (2005). Evidence for the existence of two Robo3 isoforms with divergent biochemical properties. *Mol. Cell. Neurosci.*, **30**, 485-493.

Challa, A. K., Beattie, C. E., and Seeger, M. A. (2001). Identification and characterization of roundabout orthologs in zebrafish. *Mech. Dev.*, **101**, 249-253.

Chédotal, A. (2007). Slits and their receptors. In, Bagnard, D. (ed), *Axon Growth and Guidance*. New York, NY: Springer, 65-80.

Chen, Z., Gore, B. B., Long, H., Ma, L., and Tessier-Lavigne, M. (2008). Alternative splicing of the Robo3 axon guidance receptor governs the midline switch from attraction to repulsion. *Neuron*, **58**, 325-332.

Clark, K., Hammond, E., and Rabbitts, P. (2002). Temporal and spatial expression of two isoforms of the Dutt1/Robo1 gene in mouse development. *FEBS Letters*, **523**, 12-16.

Dalkic, E., Kuscu, C., Sucularli, C., Aydin, I. T., Akcali, K. C., and Konu, O. (2006). Alternatively spliced Robo2 isoforms in zebrafish and rat. *Dev. Genes Evol.*, **216**, 555-563.

Fricke, C., Lee, J. S., Geiger-Rudolph, S., Bonhoeffer, F., and Chien, C.-B. (2001). Astray, a zebrafish roundabout homolog required for retinal axon guidance. *Science*, **292**, 507-510.

Hardy, M. E. (2010). Axon guidance and sorting in the zebrafish retinotectal system. *Diss. University of Utah*.

Hocking, J. C., Hehr, C. L., Bertolesi, G. E., Wu, J. Y., and McFarlane, S. (2010). Distinct roles for Robo2 in the regulation of axon and dendrite growth by retinal ganglion cells. *Mech. Dev.*, **127**, 36-48.

Jen, J. C., Chan, W.-M., Bosley, T. M., Wan, J., Carr, J. R., Rüb, U., Shattuck, D., Salamon, G., Kudo, L. C., Ou, J., et al. (2004). Mutations in a human ROBO gene disrupt hindbrain axon pathway crossing and morphogenesis. *Science*, **304**, 1509-1513.

Kidd, T., Brose, K., Mitchell, K. J., Fetter, R. D., Tessier-Lavigne, M., Goodman, C. S., and Tear, G. (1998). Roundabout controls axon crossing of the cns midline and defines a novel subfamily of evolutionarily conserved guidance receptors. *Cell*, **92**, 205-215.

Kimmel, C. B., Ballard, W. W., Kimmel, S. R., Ullmann, B., and Schilling, T. F. (1995). Stages of embryonic development of the zebrafish. *Dev. Dyn.,* **203**, 253-310.

Lee, J. S., Ray, R., and Chien, C.-B. (2001). Cloning and expression of three zebrafish roundabout homologs suggest roles in axon guidance and cell migration. *Dev. Dyn.*, **221**, 216-230.

Liu, Z., Patel, K., Schmidt, H., Andrews, W., Pini, A., and Sundaresan, V. (2004). Extracellular Ig domains 1 and 2 of Robo are important for ligand (Slit) binding. *Mol. Cell. Neurosci.*, **26**, 232-240.

Miyasaka, N., Sato, Y., Yeo, S.-Y., Hutson, L. D., Chien, C.-B., Okamoto, H., and Yoshihara, Y. (2005). Robo2 is required for establishment of a precise glomerular map in the zebrafish olfactory system. *Dev. Biol.*, **132**, 1283 -1293.

Park, K. W., Morrison, C. M., Sorensen, L. K., Jones, C. A., Rao, Y., Chien, C.-B., Wu, J. Y., Urness, L. D., and Li, D. Y. (2003). Robo4 is a vascular-specific receptor that inhibits endothelial migration. *Dev. Biol.*, **261**, 251-267.

Pittman, A. J., Law, M.-Y., and Chien, C.-B. (2008). Pathfinding in a large vertebrate axon tract: isotypic interactions guide retinotectal axons at multiple choice points. *Development*, **135**, 2865-2871.

Seeger, M., Tear, G., Ferres-Marco, D., and Goodman, C. S. (1993). Mutations affecting growth cone guidance in Drosophila: genes necessary for guidance toward or away from the midline. *Neuron*, **10**, 409-426.

Thisse, C., and Thisse, B. (2008). High-resolution in situ hybridization to whole-mount zebrafish embryos. *Nat Protoc*., **3**, 59-69.

Thompson, H., Andrews, W., Parnavelas, J. G., and Erskine, L. (2009). Robo2 is required for Slit-mediated intraretinal axon guidance. *Dev. Biol*., **335**, 418-426.

Ypsilanti, A. R., Zagar, Y., and Chédotal, A. (2010). Moving away from the midline: new developments for Slit and Robo. *Development*, **137**, 1939 -1952.

Yue, Y., Grossmann, B., Galetzka, D., Zechner, U., and Haaf, T. (2006). Isolation and differential expression of two isoforms of the ROBO2/Robo2 axon guidance receptor gene in humans and mice. *Genomics*, **88**, 772-778.

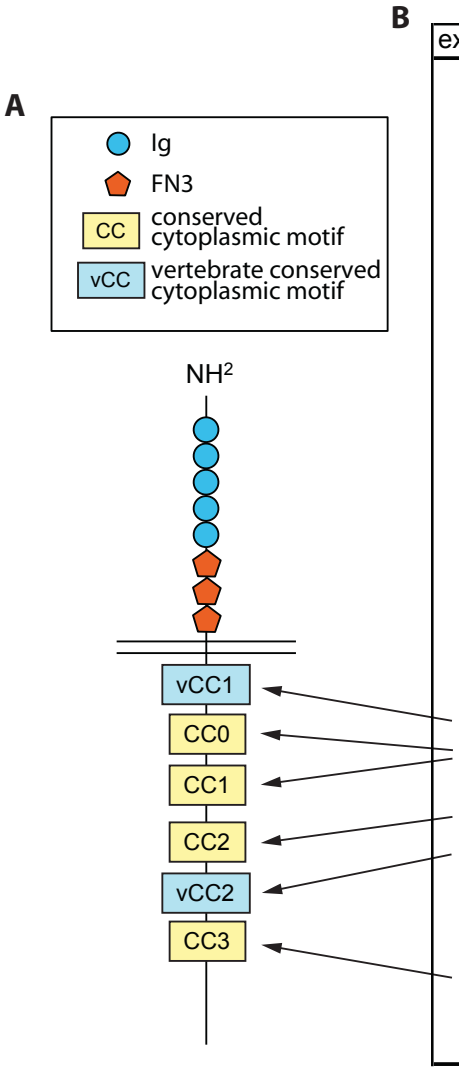

B

ex #	length	mod 3	domain	%aa sim
1	225	0	SS	74
2	327	0	Ig1	97
3	158	2	Ig2	97
4	121	1	Ig2	94
5	139	1	Ig3	94
6	137	2	Ig3	92
7	**12**	**0**	**RPVA**	**100**
8	125	2	Ig4	97
9	172	1	Ig4	96
10	206	2	Ig5	82
11	82	1	Ig5	85
12	166	1	FN1	82
13	167	2	FN1	95
14	122	2	FN2	95
15	232	1	FN2	82
16	125	2	FN3	92
17	172	1	FN3	93
18	183	0	TM	93
19	**27**	**0**		**NF**
20	43	1		92
21	122	2	vCC1	80
22	276	0	CC0/1	81
23	**126**	**0**		**97**
24	160	1	CC2	78
25	264	0	vCC2	95
26	209	2		74
27	**186**	**0**	**CAE**	**89**
28	159	0		59
29	255	0	CC3	61
30	195	0		81
31	185	2	stop	

(Adapted from Chi-Bin Chien)

Figure 3.1. Length, encoded domain, and amino acid conservation of Robo2 exons. (A) Schematic of Robo1/2 receptor structures. Not drawn to scale. (B) Each exon is listed, indicating the exon length (second column), the exon length is modulo 3 (third column), the known domains that are encoded by each exon (fourth column), and percentage amino acid similarity when compared to human Robo2 (fifth column). Three exons highlighted in red were found by our lab to be alternatively spliced. Exon 27 (highlighted in blue) is present in >= 2-week-old embryos, reported by Dalkic et al. (2007). Adapted from Chi-Bin Chien and Spencer Mangum. NF=not found; CAE=conserved alternatively-spliced exon; CC=conserved cytoplasmic domain; vCC=cytoplasmic domain conserved in vertebrates.

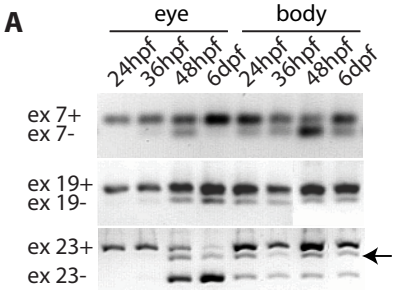

B

	Eyes				Body			
	24hpf	36hpf	48hpf	6dpf	24hpf	36hpf	48hpf	6dpf
ex7-	-	+	+	-	+	+	+	+
ex19-	-	+	+	+	+	+	+	+
ex23-	-	+	+	+	+	+	+	+

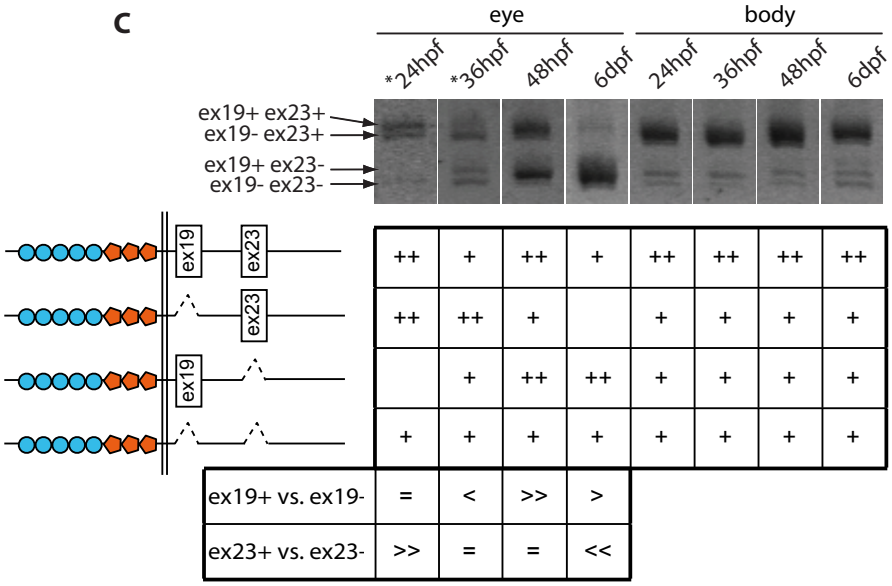

++	+	++	+	++	++	++	++
++	++	+		+	+	+	+
	+	++	++	+	+	+	+
+	+	+	+	+	+	+	+

ex19+ vs. ex19-	=	<	>>	>
ex23+ vs. ex23-	>>	=	=	<<

Figure 3.2. Analysis of spatial and temporal regulation of exons 7, 19, and 23 in developing embryos. RT-PCR from dissected eyes and remaining body tissue at 24 h, 36 h, 48 h, and 6 dpf, showing temporal and spatial regulation of ex 7, ex 19, and ex 23. (A) Exon 7 is always present in robo2 transcript but transcripts that exclude exon 7 start to appear at 36 hpf and diminish again at 6 dpf in eyes. Similarly, splice forms that include exon 19 and 23 are always present in the developing eyes but robo2 ex19- or robo2 ex23- are only present after 24 hpf. Heteroduplex band is visible for ex23 (arrow). plus sign, transcript present; minus sign, none detectable. (B) Results summarized from (A). (C) Amplicons spanning the region between exon 17 and exon 24 were amplified from cDNA of various tissue and time points to examine the linkage of different splice isoforms. Comparison between ex19+/- and ex23+/- showed that these exons are independently regulated. * = intensity increased using Photoshop. Intensity of amplicons cannot be compared across different time points. = : ex+ = ex-; » : ex+ » ex-; « : ex+ « ex-.

Table 3.1. Summary of morpholinos tested in naturally occurring alternatively spliced exons and conserved exons. Many morpholinos are toxic at doses that only induced partial exon skipping or no exon skipping at all.

endogenous alternatively spliced exons:				
ex#	length	domain		conclusions
ex 7	12bp		No exon skipping at toxic dose (tried two morpholinos)	MOs ineffective
ex 19	27bp		MO-a: Only partial exon skipping at toxic dose. Retinal axon pathfinding is normal at toxic dose. MO-d: Exon is almost completely skipped at very toxic dose. Results in no RGC differentiation but normal trigeminal ganglion development.	MOs ineffective
ex 23	126bp		MO-a: Complete exon skipping at slightly toxic dose. Delayed RGC differentiation with normal trigeminal ganglion development. MO-d: Complete exon skipping with no apparent toxicity effect. No phenotype in retinotectal pathfinding nor in CoPA axon pathfinding	exon skipping; no phenotype in RGC and CoPA axons
conserved exons (in frame deletion):				
ex 22	276bp	cc0/1	MO-a: Complete exon skipping at low dose. No retinal axon pathfinding error. MO-d: No exon skipping at high dose but causes weak astray phenotype due to in-frame deletion in exon 21.	exon skipping; not required for retinal axon pathfinding
ex 25	264bp	vcc2	MO-a: No good morpholino sequence possible. MO-d: No skipping.	MOs ineffective
ex 29	255bp	cc3	No skipping at toxic dose (tried MO-a and MO-d)	MOs ineffective

Figure 3.3. In situ hybridization of 32 hpf embryos with long robo2 riboprobes, exon 23 specific probes, and exon 22/24 probes in whole embryos and spinal cord. (A, B) Expression pattern of robo2 transcript is not altered in ex23-MOa comparing to the uninjected controls. (C, C') In situ with exon 23 specific probe shows that it is coexpressed in many regions with longer robo2 transcripts. (E, E') Transcripts without exon 23 are expressed in more restrictive patterns. (D, D') In morphants injected with ex23MO-a, expression level is significantly decreased throughout the embryos, indicating that exon 23 is skipped in the morphants. In addition, transcript level of exon 22/24 is increased in the morphants (F, F') compared to uninjected controls (E, E').

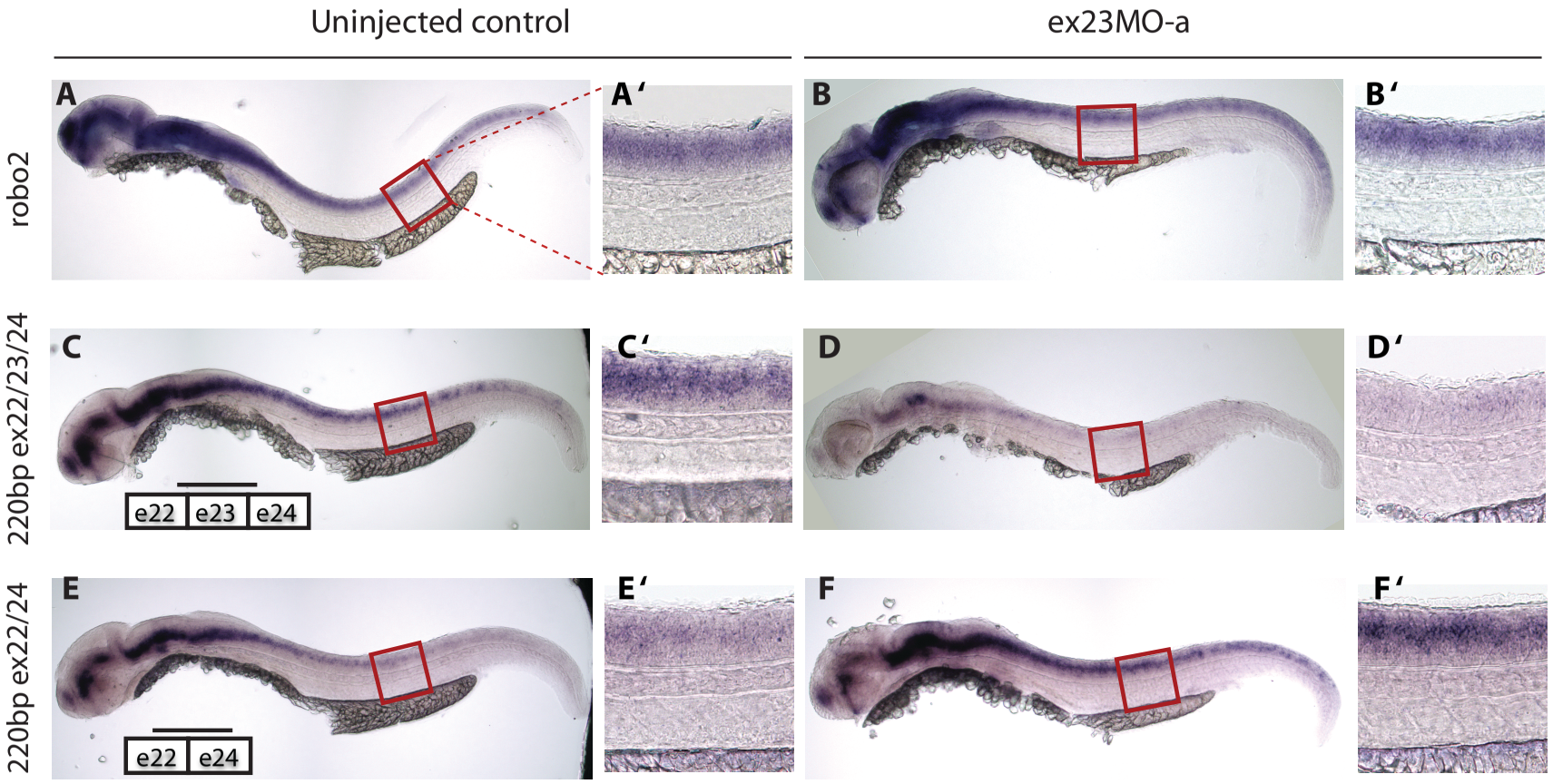
Uninjected control
ex23MO-a
robo2
220bp ex22/23/24
220bp ex22/24
A
A'
B
B'
C
C'
D
D'
E
E'
F
F'
e22
e23
e24
e22
e24

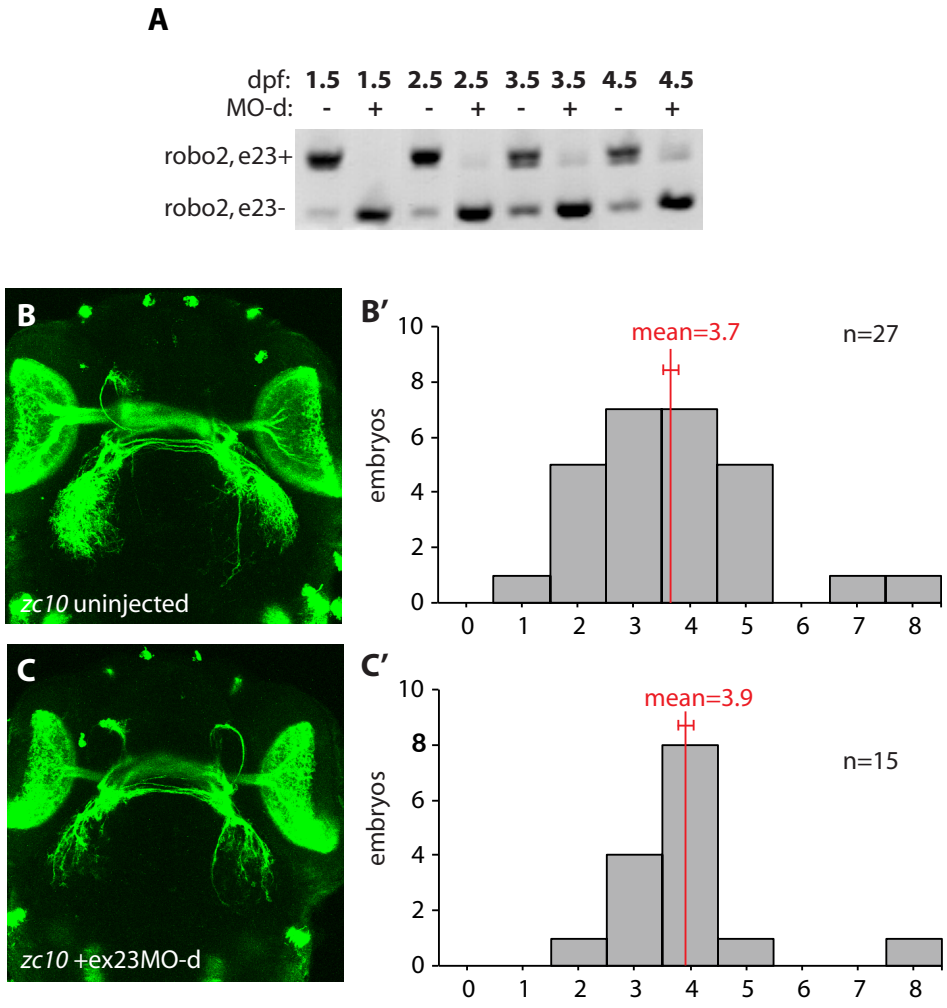

Figure 3.4. Exon 23 exclusion does not alter retinal axon pathfinding in zc10 mutants. (A) RT-PCR shows that exon 23 MO-d (12ng) can induce complete exon skipping up to 1.5 days, with a slight decline in efficiency at 2.5 dpf and onwards. (B, C) Dorsal view of 60hpf embryos, comparing zc10 mutants and ex23MO-d injected zc10 mutants. Confocal projections. (B', C') Quantification of the number of errors observed in each embryo. zc10 mutants made an average of 3.7±0.3 errors (mean±SEM) (B'). zc10 mutants injected with ex 23 MO-d score an average of 3.9±0.3 (C'). MO induced exon skipping is confirmed by RT-PCR with at least 10 embryos in each condition. X-axis represents the number of errors scored in each embryo.

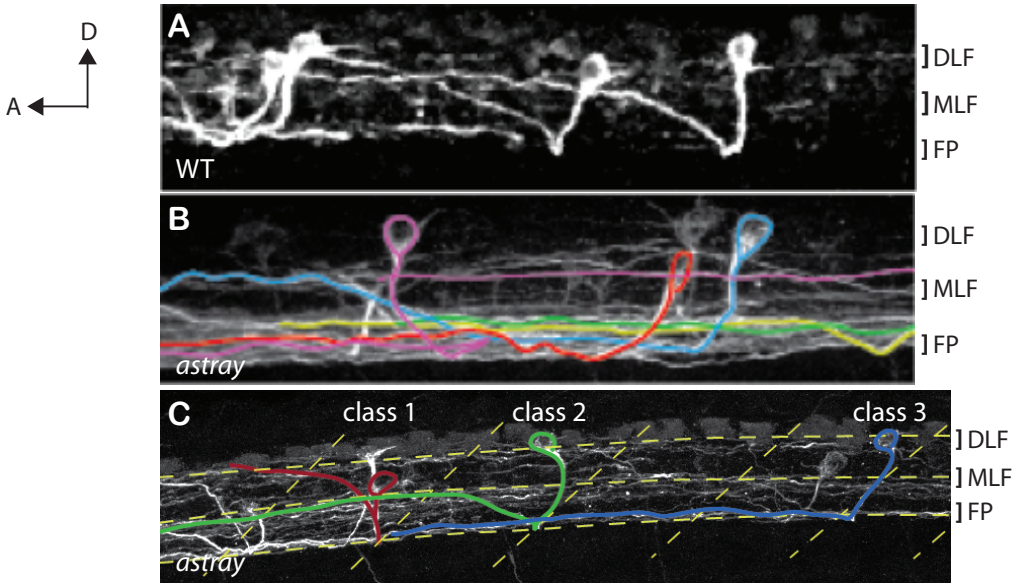

D

	class1	class 2	class 3
wt (n=24)	87.5%	4.2%	8.3%
astray mutants (n=38)	36.8%	15.8%	47.4%
ex23 morphants (n=33)	97%	3%	0%

Figure 3.5. Robo2 exon 23 is not required in CoPA axon pathfinding. (A-C) 32 hpf CoPA axons. Dorsal up, anterior to the left. (A) In wildtype, CoPA neurons are thought to extend their axons towards a Netrin gradient at the floorplate, cross the midline, then ascend dorsally, repelled by a Slit gradient at the midline. (B) In astray^{ti272z} mutants, which lack Robo2 receptor, axons cross the midline but are no longer strongly repelled by Slit and sometimes fail to ascend dorsally, travelling close to the floorplate. (C) Classification of axon trajectories. Class 1: axon is repelled from floorplate and reaches the MLF within 2 somites. Class 2: axon crosses the midline, but remains between floorplate and MLF after 2 somites. Class 3: axon stays at the floor plate after 2 somites. (D) Quantification of CoPA axon trajectory in wildtype, *astray*, and exon 23 morphants. CoPA axons in ex23MO-d morphants exhibit wildtype pathfinding. FP = floorplate. DLF = dorsal longitudinal fascicle. MLF = medial longitudinal fascicle.

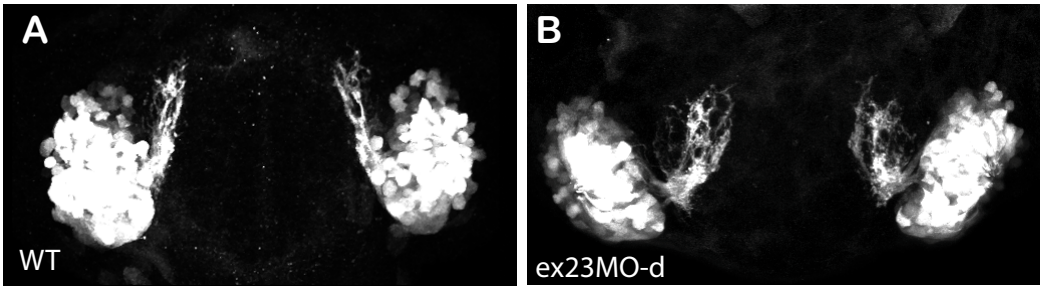

Figure 3.6. Robo2 exon 23 may be important for olfactory receptor neuron (ORN) axon pathfinding. Face-on view of ORN axons in 34 hpf omp:yfp embryos. (A) Axons from ORNs project to the olfactory bulb in a tighter bundle, compared to the morphant (B), where the tract is broader and some axons leave the main tract.

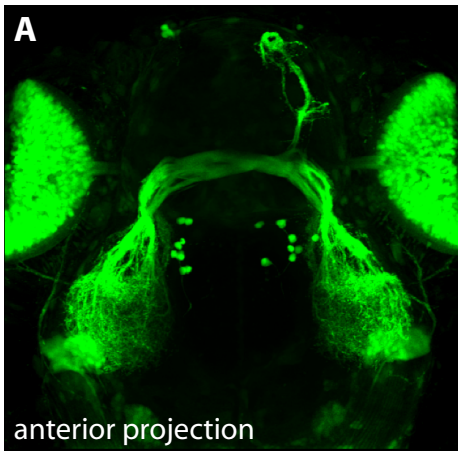

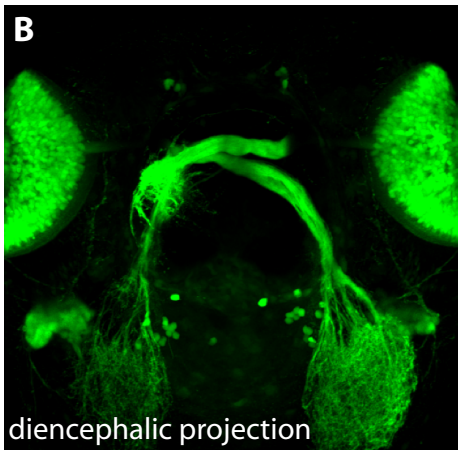

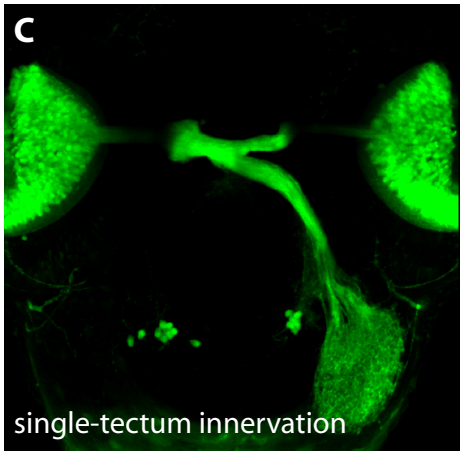

	% with errors
MO-a 1ng	0%
2ng	0%
MO-d 4ng	0%
8ng	27%
12ng	38%
16ng	55%
20ng	58%
MO-a 1ng + MO-d 8ng	22%

Figure 3.7. Exon 22 donor morpholino but not acceptor morpholino causes retinotectal pathfinding phenotype. Dorsal view of 5 dpf isl2b:GFP embryos injected with ex22MO-d. Three classes of pathfinding errors that are often found in morphants include anterior projection (A), diencephalic projection (B), and single-tectum innervation (C). (D) MO-a effectively induces clean skipping of exon 22 but does not cause any pathfinding phenotype in morphants at its toxic dose (2ng). MO-d causes partial phenotype in isl2b:GFP transgene labelled retinal axons. Rate of pathfinding error increases with MO-d dosage. Combination of MO-a and MO-d does not increase phenotype penetrance. n=12-57 embryos per condition.

CHAPTER 4

DISCUSSION

Summary

Given the complex nature of brain wiring, I find it surprising and highly gratifying that axonal connection occurs in an automatic fashion, with minimal hiccups in most individuals. Most of us take for granted the axon navigation and targeting that happen in such a spontaneous and mysterious way. With the advances in biological technologies and tools available, many guidance cues have been discovered and many of their functions revealed. However, taking what is published about each molecule and piecing all the information together remains a big challenge.

In this dissertation, I describe the role played by pioneer-follower interactions when put in conflict with the absence of an important retinal axon guidance signal. Prior to this work, the role of pioneer axons had often been tested in simple systems, usually with mechanical perturbation. I showed that in a large vertebrate tract in vivo, pioneer axons and Robo2 signaling have an equally important role in follower axon navigation in the brain when axons are directly interacting with each other (peer axons). Robo2 functions have a predominant effect in follower axon guidance. On the other hand, Robo2 plays an important role in the RGC axon at multiple choice points along its path from the retina to the tectum. How a single *robo2* gene has different functions is not well understood. Another section of my work describes the regulation and function of *robo2*

alternate splice forms in the retina and other parts of the nervous system. Therefore, my work adds to our understanding of the complexities of vertebrate axon guidance.

Axon-axon interaction in retinotectal guidance

Axon guidance by both ligand-receptor complexes and pioneer-follower axon interaction has been widely studied. It began in 1963 when Roger Sperry proposed the chemoaffinity model which stated that particular chemical cues might be recognized specifically by chemical receptors (Sperry, 1963). About 10 years later, research in freshwater fleas suggested another mode of guidance: axons can be guided by other axons that have grown earlier through the same tract (pioneer axons) (Lopresti et al., 1973). Since then, many guidance molecules have been identified molecularly (see Chapter 1) and the roles of pioneer axons have been studied further (Chapter 2). Previous studies of axon guidance have focused on how ligand-receptor complexes or pioneers guide axons, but have not tested the effect of both on the same type of axons. Pioneer axon experiments have mostly been carried out in simple systems where only a small number of axons are traveling together. In addition, mechanical ablation of pioneer axons can potentially alter the environment. Therefore, it remained unclear how these two factors interact and affect axon pathfinding in a large vertebrate tract. Our results (Chapter 2) are the first to describe, in an intact environment, the effect of pioneer-follower interaction on axon navigation of a large axon tract. They suggest that the interaction between pioneer and follower axons can be as important as guidance molecules in axon navigation.

Are axons affected by other axons traveling along the same path? Results from our transplant experiments show that the genotype of host embryos can strongly affect

donor axon navigation (Appendix). For instance, wildtype donor RGCs transplanted into an *astray* host make similar types of pathfinding errors (although fewer) as *astray* RGC axons. However, we also know that Robo2 acts eye-autonomously (Fricke et al., 2001). In other words, the genotype of the host brain environment does not affect retinal axon navigation. Thus, our results strongly suggest that peer axons provide guidance cues that guide peers. The mechanisms that mediate peer-peer and pioneer-follower interactions is not well understood; what distinguishes the pioneers from the rest of the tract is also not known. An obvious next step will be to confirm the hypothesis that followers are indeed guided by pioneers in retinotectal guidance. I have made another transgenic fish line, *isl2b:tagRFP*, for this purpose. This allows us to carry out live imaging of retinal axon growth in transplanted host embryos, in which donor and host RGCs are labeled with different transgenes.

What mediates pioneer-follower interactions? Cell adhesion molecules (CAMs) expressed in the retina are the most likely candidates to regulate axon-axon fasciculation. As discussed previously in Chapter 1, several CAMs from the Ig-superfamily are known to be expressed in the retina or are implicated in retinal axon guidance: NCAM, NrCAM, L1.1, L1.2, Neurolin, and NLCAM. Based on data in the Appendix, NCAM and neurolin are expressed in the retina at about 37 hpf. We can test the functions of these molecules in pioneer-follower interactions with morpholinos or with mutants. If several CAMs are expressed simultaneously in retinal axons, it may be necessary to knock down several at once to disrupt retinal axon interaction in vivo. Adhesive properties of NCAM can be modified by sialic acid modification that creates steric hindrance between NCAM interactions. I have tried to express sialyltransferase in the retina that is important in

adding sialic groups to NCAM. However, this strategy does not yield expected results in disrupting axon fasciculation, likely due to the poor availability of sialic acid in younger retina.

Alternate splicing of Robo2

Robo2 has multiple roles in RGC guidance. It is required for mouse intraretinal guidance (Thompson et al., 2009), Xenopus dendritic extension and branching and axon extension (Hocking et al., 2010), guidance at the optic chiasm (Fricke et al., 2001), guidance in the optic tract (Hardy, Ph.D. dissertation), and axon arborization and stabilization in the tectum (Campbell et al., 2007). This leads to the question, how does Robo2 respond differently in various biological processes? In addition, many Robo-interacting molecules have been described from work either in Drosophila or in vitro, but their functions in vertebrate systems have not been described. My work in Chapter 3 described up to nine *robo2* splice isoforms that are temporally and spatially regulated during early zebrafish development. Alternative splice forms can significantly increase protein diversity and function, in this case generating 9 polypeptides from a single gene. These experiments began an effort to understand roles of different Robo2 alternate splice forms during axon growth. Using morpholinos specifically targeted to induce exon skipping, I tried to correlate conserved Robo2 motifs with in vivo functions of axon pathfinding. An alternatively spliced exon (exon 23) does not have a role in retinal or CoPA axon pathfinding. Interestingly, my preliminary results showed that this exon may be important in directing axons from the olfactory receptor neurons to reach their target correctly. In addition, I showed that two conserved domains, CC0 and CC1, are not

responsible for retinal axon guidance in vivo. This result is surprising because these two motifs are very conserved from invertebrate to vertebrate.

Testing the functions of Robo2 conserved motifs in zebrafish can help us to test whether Robo-interacting proteins function in vertebrate axon guidance in vivo. Morpholino experiments provide a quick method to study gene functions but have their own limitations. In particular, many morpholinos have toxic or off-target effects, and many fail to inhibit splicing as desired. Another approach would take advantage of the available Robo2 null mutants (*astray*^{ti272z}), together with strong promoters that drive in all RGCs (*islet2b*). By carrying out rescue experiments by overexpressing slightly modified *robo2* constructs in *astray*^{ti272z}, we should in theory be able to understand the functions of these constructs in retinal axon guidance. I have tried multiple methods to express the 4.8kb *robo2* cDNA transiently but so far none has worked well enough. *Robo2* is long. Its genomic sequence spans up to 0.36 mega bases with long intron sequences. It is not clear whether the intron sequences house regulatory sequences that affect expression. It is possible that *robo2* intron sequences may regulate transcription or translation of the gene. Further experiments to determine the limiting steps in *robo2* overexpression are needed. Also, *robo2* expression in transiently expressing embryos is very mosaic. Expression can likely be improved in stable transgenics, but this requires laborious experiments.

Overall, my work in pioneer-follower guidance has advanced our understanding of the collaborative effort between axon-axon interaction and traditional guidance cues in guidance of a large vertebrate tract. I have also opened the door for further study of the role of *robo2* alternate splice forms in regulating different decisions (choice points) during axon pathfinding.

Reference

Campbell, D. S., Stringham, S. A., Timm, A., Xiao, T., Law, M.-Y., Baier, H., Nonet, M. L., and Chien, C.-B. (2007). Slit1a inhibits retinal ganglion cell arborization and synaptogenesis via Robo2-dependent and -independent pathways. *Neuron*, **55**, 231-245.

Fricke, C., Lee, J. S., Geiger-Rudolph, S., Bonhoeffer, F., and Chien, C. B. (2001). Astray, a zebrafish roundabout homolog required for retinal axon guidance. *Science*, **292**, 507-510.

Hocking, J. C., Hehr, C. L., Bertolesi, G. E., Wu, J. Y., and McFarlane, S. (2010). Distinct roles for Robo2 in the regulation of axon and dendrite growth by retinal ganglion cells. *Mech. Dev.*, **127**, 36-48.

Lopresti, V., Macagno, E. R., and Levinthal, C. (1973). Structure and development of neuronal connections in isogenic organisms: cellular interactions in the development of the optic lamina of Daphnia. *Proc. Natl. Acad. Sci. U.S.A.*, **70**, 433-437.

Sperry, R. W. (1963). Chemoaffinity in the orderly growth of nerve fiber patterns and connections. *Proc. Natl. Acad. Sci. U.S.A.*, **50**, 703-710.

Thompson, H., Andrews, W., Parnavelas, J. G., and Erskine, L. (2009). Robo2 is required for Slit-mediated intraretinal axon guidance. *Dev. Biol.*, **335**, 418-426.

Wilson, S. W., Ross, L. S., Parrett, T., and Easter, S. S., Jr (1990). The development of a simple scaffold of axon tracts in the brain of the embryonic zebrafish, Brachydanio rerio. *Development,* **108**, 121-145.

A

- ath5MO	WT > WT 0 error	WT > ast 2.7 errors	ast > ast 7.9 errors	ast > WT 2.9 errors
+ ath5MO	WT > WT; ath5MO 0 error	ast > WT; ath5MO 1.7 errors	Ast > ast;ath5MO 6.0 errors	WT > ast;ath5MO 4.8 errors

B

	Pioneer - follower	Peer - peer
Inside eye	Strong	N.D.
After exiting eye	Weak	Strong

Figure 4.1. Result summary from transplant experiments. (A) In regular cell transplant experiments, retinal axons from donor cells appear to be affected by the genotype of its host. When donor cells are transplanted into host embryos injected with ath5MO, axon from later-born (donor) RGCs are moderately affected by pioneer retinal axons. (B) Result summary from transplant experiment inside and outside the eye. Pioneer-follower effect is strong among retinal axons within the eye but is weaker once they exit the eye. When traveling outside of the eye, peer-peer interaction between axons has a strong effect on axon trajectory. N. D.= not determined.

APPENDIX

In Chapter 2, we showed that axon fasciculation plays an equally important role as other guidance cues during retinal axon outgrowth in the brain. However, it is not clear which cell adhesion molecule (CAM) is crucial for RGC axons to pathfind between the retina and the tectum. It is also likely that more than one CAM is present in the retinal axons. In this appendix, I examine the expression pattern of several known members from the immunoglobulin superfamily cell adhesion molecules (IgCAMs) that have either been shown to be expressed in the retina or affect some aspects of retinal axon navigation in some vertebrate species: NCAM, L1.1, L1.2, neurolin, NLCAM, and NrCAM (Figure A1).

Figure A1. Expression patterns of NCAM, L1.1, L1.2, NrCAM, neurolin, and NLCAM in dorsal views of the retina from 24 hpf to 77 hpf. Medial to left, lateral to right, anterior up. (R) is a lateral view of the retina. (A-D) At 24 hpf, NCAM expression is homogenous in the retina at all time points examined, with very low expression at 77 hpf. (E-L) L1.1 (E-H) and L1.2 (I-L) are expressed in the brain but not the retina at 24 and 37 hpf. Their expression increases in and localizes to the RGC layer at 50 and 77 hpf. (M-P) NrCAM expression is not present or present at a very low level in the retina from 24 hpf to 77 hpf. There is staining in the brain (not shown) and in the lens from 24-48 hpf. (Q-T) Neurolin is expressed throughout the retina at 24 and 37 hpf but can be seen to be more highly expressed in the ventral-nasal part of the retina, where RGC differentiation begins (R). Expression is highly restricted to the RGC layer at 50 and 77hpf. (U-X) NLCAM expression is restricted to the RGC layer at 50 hpf and shows weak homogenous expression at 24 and 37 hpf. Expression of all six CAMs is excluded from the ciliary marginal zone.

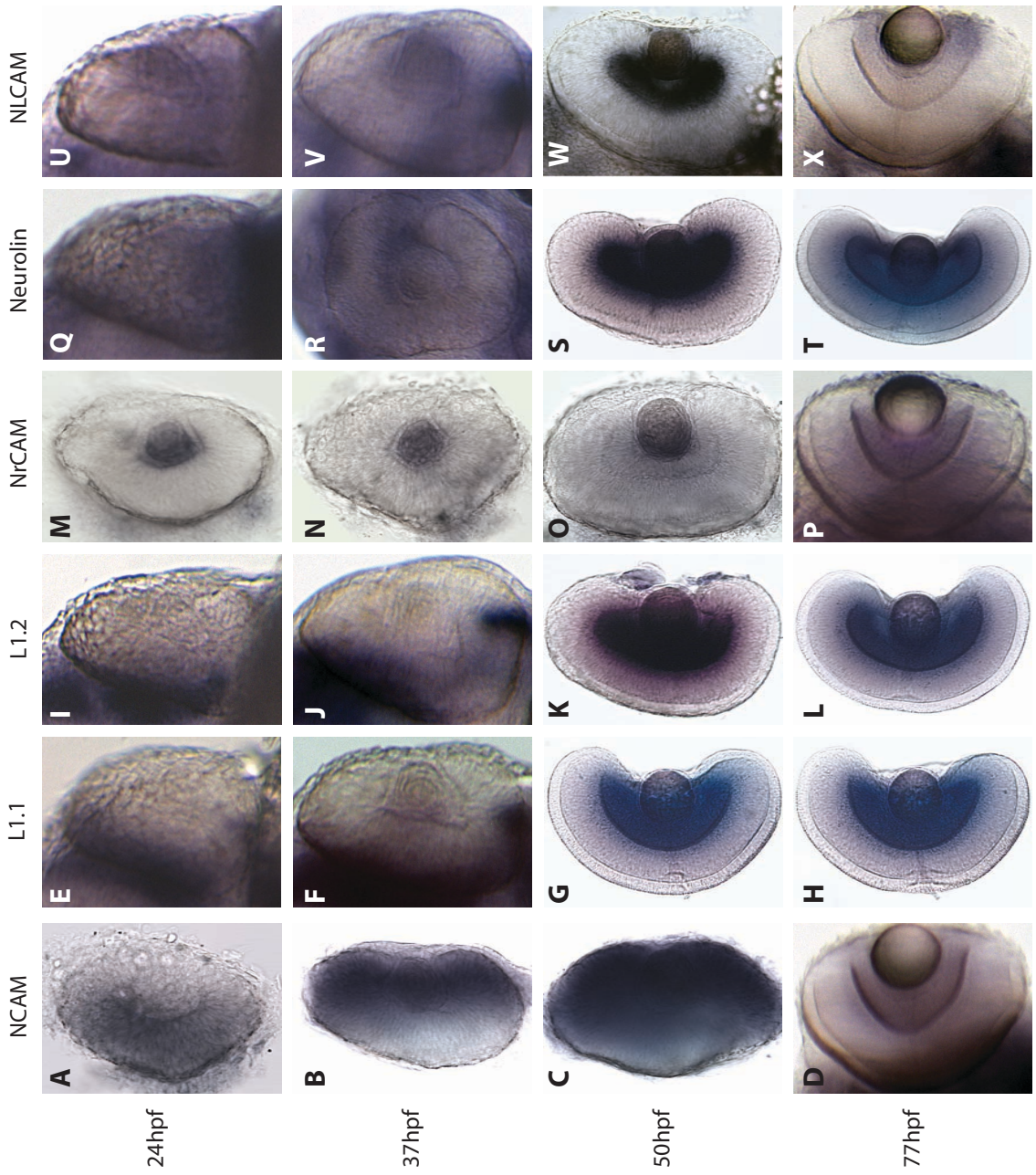
NCAM
L1.1
L1.2
NrCAM
Neurolin
NLCAM
24hpf
37hpf
50hpf
77hpf
A
B
C
D
E
F
G
H
I
J
K
L
M
N
O
P
Q
R
S
T
U
V
W
X